STATIC ANALYSIS OF LAMINATED COMPOSITE PLATES USING FINITE ELEMENT METHOD

by

NAGARAJA, K. S.

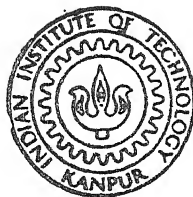# STATIC ANALYSIS OF LAMINATED COMPOSITE PLATES USING FINITE ELEMENT METHOD

A Thesis Submitted
in Partial Fulfilment of the Requirements
for the Degree of
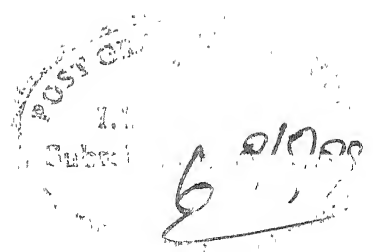*MASTER OF TECHNOLOGY*

by

NAGARAJA, K. S.

to the

DEPARTMENT OF AEROSPACE ENGINEERING

INDIAN INSTITUTE OF TECHNOLOGY, KANPUR

MAY, 1989

CERTIFICATE

This is to certify that the work "STATIC ANALYSIS OF LAMINATED COMPOSITE PLATES USING FINITE ELEMENT METHOD" has been carried out under my supervision and any part of this work has not been submitted elsewhere for a degree.

(S. Kamle)
Assistant Professor
Department of Aeronautical Engineering
Indian Institute of Technology
Kanpur-208016

May, 1989

ACKNOWLEDGEMENTS

CONTENTS

LIST OF TABLES

LIST OF FIGURES

ABSTRACT

A higher order shear deformation theory is used to carry out the stress and stability analysis of laminated composite plates. A displacement based finite element formulation using a isoparametric, 9-noded, lagra-ngian element is employed. A finite element buckling formulation for the higher order theory is developed and presented. Separate formulations are done for symmetric and unsymmetric laminates to achieve computational efficiency. A FORTRAN program is developed to efficiently implement the formulation. Numerous examples drawn from available literature are solved to emphasize the reliabilit of the formulation and program. The results are presented in the form of tables and graphs.

CHAPTER 1

INTRODUCTION AND LITERATURE REVIEW

1.1 Introductory Remarks

The fibre reinforced composites are being increasingly used as load bearing structural members in aeronautical, automobile, marine, civil and other fields of engineering. This is due to the superior mechanical properties possessed by these materials. A composite material offers a significant weight reduction in a structure in view of its high strength to weight and high stiffness to weight ratios. Also, in fibrous composites the mechanical properties can be varied by suitably varying the orientation of the fibres. Other advantages include improved fatigue life, wear resistance, corrosion resistance, temperature dependent behaviou etc.

A fibrous composite material essentially consists of high strength fibres embedded in a matrix. The most common types of fibres that are in use include glass, carbon, graphite, boron, silicon carbide, kevlar, etc. A few of the matrix materials being used are epoxy phenolics, polyesters, etc.

A lamina is a thin sheet with fibres oriented in a certain direction forming the main load bearing members. The matrix is characterized by a low modulus and high elongation and it transfers stress to the fibres through bonding at the fibre-matrix interface. It keeps the fibres in position, provides flexibility and protects the fibres from the environment. A lamina can be basically considered to be homogeneous, two-dimensional and orthotropic.

A laminate consists of a number of laminae bonded together. The anisotropic behaviour of a laminate can be tailored through the variation of laminae stocking sequence and fibre orientation. This feature gives additional degree of flexibility to the designer while simultaneously posing unique challenges to the analyst. The extensional modulus along the fibres is usually very large relative to the extensional modulii in the lateral directions and the trans-verse shear modulii, due to the differences in elastic pro-perties between fibre filaments and matrix materials. This is a marked departure from conventional isotropic materials. Consequently, the relative importance of physical effects is influenced by the directional nature of properties and their relative magnitude.

Due to the relatively low transverse shear modulii, the shear deformations are much significant in fibre rein-forced composites. Further the delamination mode of failure

is initiated due to interlaminar stresses. The inplane
stresses govern the strength requirements. The buckling
phenomenon becomes important for aircraft panels made of
composite materials, as the buckling of the skin affects the
aerodynamic characteristics giving rise to inadmissible drag
at high speeds. Therefore, an accurate prediction of the
structural response with regards to strength and stability
becomes imperative.

1.2 Literature Review

The classical laminate theory, which is an extension of
the classical plate theory to laminated plates, ignores the
transverse stress components. The first complete laminated
anisotropic plate theory is attributed to Reissner and
Stavsky [1]. The classical laminate theory is adequate only
for very thin plates.

An adequate theory for laminates must account for
accurate distribution of transverse shear stresses. Many
theories which account for the transverse shear and normal
stresses are available in literature, prominent among them
being that of Mindlin [2] and Reissner [3]. A generalization
of the first order shear deformation theory for homogeneous
isotropic plates to laminated anisotropic plates is due to
Yang et al. [4]. Whitney and Pagano [5] extended the YNS
theory [4] to laminates consisting of arbitrary number of

bonded anisotropic layers. In this theory, the normals to
the midplane before deformation remain straight but not
necessarily normal to the midplane after deformation. Con-
sequently, a correction to transverse stiffnesses is require
The shear correction coefficient depends on constituent ply
properties, ply lay up, fibre orientation and the particular
application. Reddy [6] used a C^o penalty plate bending
finite element for the solution of the governing equations
of YNS theory. The displacements (u, v, w) and midplane
rotations (ψ_x, ψ_y) were independently interpolated and
coupled via the shear energy terms which behave as penalty
terms that restrict the shear rotations to zero at thin
plate limits. Subsequently, Reddy [7] presented a compari-
son of the finite element solutions using the penalty method
and exact closed form solutions, for thick anisotropic
rectangular plates. The effects of reduced integration,
mesh size and element type on the accuracy of the penalty
finite element were investigated. He concluded that the
9-noded Lagrangian element is not affected by integration
scheme while the 8-noded element is profoundly affected.
The consideration of symmetry in the analysis of unsymmetri-
cally laminated anisotropic plate was studied by Reddy [8].
The equilibrium equations for a lamina were used by Engblom
and Ochoa [9] to arrive at a more accurate prediction of the
transverse shear stresses. Equations were written in terms

of differences in stresses across a lamina, analogous to the
equilibrium equations. Thus a set of simultaneous equations
were obtained considering all the laminae and solved.

The deflection analysis of hybrid laminated rectangular
and skew composite plates was conducted by Iyengar and
Umaretiya [10]. They used the Galerkin rechnique to obtain
numerical results for Kevlar/epoxy and Boron/epoxy laminates.
It was observed that for a given aspect ratio, an increase
in skew angle increased the rigidity of the skew plate. They
also concluded that for a specified deflection, the hybrid
laminates are lighter. Haas and Lee [11] used a nine-noded
degenerate solid shell element based on modified Hellinger-
Reissner principle. Functions were assumed independently
for inplane and transverse shear strains. Stress smoothing
was adopted by Owen and Li [12] to overcome the discontinuit
of transverse shear stresses.

Further developments in laminate analysis have been
higher-order theories. 'Higher order' denotes a variation of
displacement that is higher than linear through the laminate
thickness. A discussion of these theories appears in Ref.12
Lo et al. [12,13] and Reissner [14] presented theories for
plates based on assumed higher order displacement field. The
displacement field proposed by Lo et al. incorporate inplane
modes of deformation in the displacement field of Reissner.
A higher order theory which not only accounts for transverse

shear deformation but also satisfied the zero shear stress conditions on the top and bottom faces of the plate was suggested by Reddy [15]. Phan and Reddy [16] presented a finite element formulation of the higher order theory in which inplane displacements are expanded as cubic functions of the thickness coordinate while the transverse deflection is kept independent of the thickness coordinate. The contributions and effects of transverse normal stress and strain are neglected. Putcha and Reddy [17] developed a mixed shear finite element based on the higher order theory. The element consists of eleven degrees of freedom per node, i.e., three displacements, two rotations and six moment resultants.

The transverse shear stresses and inplane displacements are considered to be continuous between layers in Ren's theory [18]. He obtained closed form solution for anti-symmetric laminates. Krishnamurthy [19] assumed a displacement field which leads to parabolic inplane stresses but neglects transverse normal stress. The condition of zero transverse shear on top and bottom free surfaces was satisfied. Later [20] he used cubic inplane and parabolic transverse displacements to obtain closed form solution for a symmetric four-layered infinite strip. He observes that 'statically equivalent' estimates of interlaminar stresses display the required interface continuity and agree very closely with exact solutions. Vijaykumar and Krishnamurthy [21] presented an 'iterative modelling' in which displacement

field is successively generated by utilising the displace-
ment field of immediately previous lower order theory. This
implements the higher order theories in a hierarchial fashion
Librescu and Khdeir [22] employed the state space concept to
obtain solutions for governing equations of Reddy's type
higher order theory. The effect of various boundary condi-
tions was investigated. Kant [23] based his higher order
shear deformation theory on the Taylor's series expansion
of generalized displacements. He used a new approach for
satisfying zero transverse shear conditions on top and
bottom bounding planes. A variety of models based on vary-
ing assumptions for the displacement fields have been deve-
loped and tested for accuracy.   A displacement based C^o
finite element formulation was presented.

The finite element formulation of the plate buckling
problem is available in standard texts, such as that of
Zienkiewicz [24] and Cook [25] and various papers [26,27,
28]. The buckling of multilayer plates has been dealt with
by Lunggren and Salama [29] using the finite element method.
Buckling analysis of composite plates has been discussed
in Iyengar's text [30]. Jones [31] obtained closed form
solutions for the buckling and vibration of unsymmetric
cross ply laminated plates. A method for incorporating the
curvature terms in the nonlinear strains used in developing
the initial stress matrix is given by Whitney [32]. He

concludes that curvature terms have little effect on the critical buckling loads for the symmetric laminates that were investigated.

The vibration and stability and symmetrically laminated composite plates were studied by Dawe and Craig [33] using the finite strip and Rayleigh Ritz method. Owen and Li [34] used the heterosis element for the vibration and stability analysis of laminated plates. Recently, Gajbir Singh and Sadasiva Rao [35] used a 8-noded element with five degrees of freedom per node for the stability analysis of thick angle ply composite plates. They use all the components of the nonlinear strains and the initial stress matrix is obtain ed by carrying out the stress analysis. The effects of fibre orientation, material properties, layering and boundary conditions on buckling load are studied.

Phan and Reddy [36] used the Reddy's higher order theory to obtain closed form solutions for the stability of isotropic, orthotropic and laminated plates. A mixed element based on the same theory is developed by Putcha and Reddy [37]. Doong [38] adopts a higher order theory for the vibration and stability of an initially stressed laminated plate. He compares the results with Reddy's [36] closed form solutions. Khdeir [39] exactly solves the higher order governing equations developed by Reddy, by making use of the generalized Levy's type solution in conjunction with the state space

concept. He obtains uniaxial critical buckling loads for symmetric cross ply laminates for varying boundary conditions. Subsequently, [40] he used his higher order theory to analyse the free vibration and buckling of unsymmetric cross ply laminates. Recently, Ren [41] obtained results for vibration and buckling analysis of simply supported, unsymmetric, cross ply and angle ply laminates. His theory allows for parabolic distribution of transverse shear stress which are continuous across the interface.

A review of the different approaches used for modelling multilayered composite plates is recently published by Noor and Burton [42]. The discussion focusses on the approaches for developing two-dimensional shear deformation theories.

1.3 Objective and Scope of the Present Work

The literature review reveals the following facts prompting and influencing the course of the present work :

*   A very few displacement based finite element adoptions of the higher order theory are available in the literature. This necessitates the assessment of the reliability and accuracy of such a formulation for varied physical conditions and material parameters. This becomes all the more imperative due to the simplicity and versatality of the finite element method for use in practical problems.

*   A   comparative study of the numerical results
obtained from two or more higher order theories in order to
establish their relative predictive capabilities has never
been taken up.

*   The adaptability of a formulation for laminated compo-
sites to the analysis of sandwich plates has been rarely
tested.   And except for Kant [23], none seems to have
approached the sandwich plate problem through the higher
order theory.   Hence, this area remains largely unexplored
and untested.   For example, the consideration of shear
rigidity of faces needs to be thoroughly examined.

*   Formulation of a higher order theory for the buckling
of laminated composites using the finite element method is
attempted   in only one or two papers [37].   Further, the
displacement based formulation for the same seems untouched.

    In the light of the above observations, an attempt has
been made in the present work to analyze the bending and
buckling response of laminated composite plates.   The higher
order theory proposed by Tarun Kant [23] forms the basis for
the present study.   The displacement based finite element
method using a C^o, isoparametric, lagrangian, quadrilateral
element is employed.   A consistent formulation for the buck-
ling analysis is devised and presented.   The results are

obtained for a variety of examples chosen from available
literature which cater for the variation of a number of
parameters. Transverse shear stresses are evaluated using
constitutive relations as well as equilibrium equations.
The application to the stress analysis of sandwich plates is
extensively investigated. The results are compared with
those from first order shear deformation theory and classi-
cal plate theory in order to determine the range of applica-
bility and necessity of each. The present results are also
compared with the results from other higher order theories,
particularly closed form solutions.

Formulations are presented separately for symmetric and
unsymmetric laminates in view of the computational efficiency
achieved thereby. A program is developed in FORTRAN for the
computer implementation of the formulations.

CHAPTER 2

THEORETICAL FORMULATION

2.1 Preliminary Remarks

This chapter presents a detailed formulation of a higher order shear deformation theory for the bending and buckling analysis of laminated composite plates. The displacement field is chosen in a series form. The governing equations are developed entirely in terms of the displacement at the midplane. Strains and stresses are obtained from displacements using strain-displacement and constitutive relations. The development of the theoretical formulations for symmetric and unsymmetric laminates are presented side by side.

2.2 Assumptions made in the Analysis

(a) Displacements and strains are small and linear elasticity theory applies.

(b) The transverse normal stress and strain are negligible.

(c) The points on the normal to the reference surface before deformation need not remain on a straight line after deformation.

The assumption (c) is the basis for any higher order theory. It implies a nonlinear variation of the inplane displacements through the plate thickness.

2.3 Definition of the Displacement Field

The displacement field chosen is such as to approximate the 3-dimensional elasticity problem by a 2-dimensional plate problem. This involves the expansion of the displacement components (u,v,w) at any point in the plate in a Taylor's series in terms of the coordinate normal to the reference surface, 'Z'. The inplane displacements are expanded as cubic function of thickness coordinate while the transverse deflection is assumed to be constant throughout the thickness This is in accordance with the assumptions (b) and (c). The displacement field is defined as :

$$u(x,y,z) = u(x,y,o) + z(\frac{\partial u}{\partial z})_0 + \frac{1}{2!} z^2 (\frac{\partial^2 u}{\partial z^2})_0 + \frac{1}{3!} z^3 (\frac{\partial^3 u}{\partial z^3})_0$$

$$v(x,y,z) = v(x,y,o) + z(\frac{\partial v}{\partial z})_0 + \frac{1}{2!} z^2 (\frac{\partial^2 v}{\partial z^2})_0 + \frac{1}{3!} z^3 (\frac{\partial^3 v}{\partial z^3})_0$$

$$w(x,y,z) = w(x,y,o) \quad , \tag{2.1}$$

where x,y and z represent the coordinate axes of the plate.

The expansions of the inplane displacements (u,v) accommodate the warping of the transverse cross-section. Certain terms in the expansions of the displacements given by

Eqns. (2.1) correspond to the membrane behaviour while others represent the flexure behaviour. The two contributions can be grouped and written as follows :

<div style="text-align:center">membrane part   flexure part</div>

$$u = u_o + z^2 u_o^* \qquad\qquad + z\,\Theta_x + z^3\,\Theta_x^*$$

$$v = v_o + z^2 v_o^* \qquad\qquad + z\,\Theta_y + z^3\,\Theta_y^*$$

$$w = \qquad\qquad\qquad\qquad w_o \qquad\qquad (2.2a)$$

where, $u_o = u(x,y,o)$; $v_o = v(x,y,o)$ and $w_o = w(x,y,o)$ are the displacements at the midplane, $\Theta_x = (\frac{\partial u}{\partial z})_o$; $\Theta_y = (\frac{\partial v}{\partial z})_o$ are rotations of the normals to the midplane about y and x axes respectively. The parameters (u_o^*, v_o^*) and (Θ_x^*, Θ_y^*) are the higher order terms in the Taylor's series defined at midplane. They can be identified as the higher order contributions to the inplane displacements and rotations respectively.

For symmetric laminate, the midplane of the plate represents the neutral surface during deformation. Thus, when only transverse loading is considered, the membrane parts can be dropped from Eqns. (2.2a) to yield a simplified versio of the displacement field for such class of laminates, viz.,

$$u = z\,\Theta_x + z^3\,\Theta_x^*$$

$$v = z\,\Theta_y + z^3\,\Theta_y^*$$

$$w = w_o \qquad\qquad\qquad\qquad (2.2b)$$

The geometry of a laminate plate with assumed positive set of coordinates and physical midplane displacements is shown in Figure 2.1. The lamina reference axes are also defined.

2.4 Stress-Strain Relations for an Orthotropic Lamina

Each lamina of a composite structure is treated as homogeneous and orthotropic. A laminate is formed by bonding together a number of such laminae.

Noting the assumption that w is constant across the thickness of the lamina and that normal stress $\sigma_3 = 0$, the stress-strain relationship is obtained. Thus, the stress-strain relationship with reference to the principal material axes for an orthotropic lamina can be written as,

$$
\begin{Bmatrix} \sigma_1 \\ \sigma_2 \\ \sigma_{12} \\ \sigma_{23} \\ \sigma_{13} \end{Bmatrix}^L
=
\begin{bmatrix}
\dfrac{E_1}{1-\nu_{12}\nu_{21}} & \dfrac{\nu_{21} E_1}{1-\nu_{12}\nu_{21}} & 0 & 0 & 0 \\[2mm]
\dfrac{\nu_{12} E_2}{1-\nu_{12}\nu_{21}} & \dfrac{E_2}{1-\nu_{12}\nu_{21}} & 0 & 0 & 0 \\[2mm]
0 & 0 & G_{12} & 0 & 0 \\[2mm]
0 & 0 & 0 & G_{23} & 0 \\[2mm]
0 & 0 & 0 & 0 & G_{13}
\end{bmatrix}^L
\begin{Bmatrix} \epsilon_1 \\ \epsilon_2 \\ \gamma_{12} \\ \gamma_{23} \\ \gamma_{13} \end{Bmatrix}^L
$$

or, concisely, $\sigma' = \bar{C}\epsilon'$ (2.3)

In general, it may be required that each lamina has its principal material axes oriented at a different angle with

respect to the laminate reference system of axes. This necessitates the transformation of the above constitutive relations from the lamina axes (1,2,3) to the laminate reference axes (x,y,z). This transformation is done using the relation,

$$Q = T^{-1} \, \bar{C} \, [T^{-1}]^T \tag{2.4}$$

where the transformation matrix T is defined as,

$$T = \begin{bmatrix} C^2 & S^2 & -2SC & O & O \\ S^2 & C^2 & 2SC & O & O \\ SC & -SC & C^2-S^2 & O & O \\ O & O & O & C & -S \\ O & O & O & S & C \end{bmatrix} \tag{2.5}$$

in which $C = \cos\alpha$ and $S = \sin\alpha$.

The triple product defined by Eqn. (2.4), now relates the stresses and strains for an orthotropic lamina with reference to the laminate reference system of axes, given as,

$$\begin{Bmatrix} \sigma_x \\ \sigma_y \\ \sigma_{xy} \\ \sigma_{yz} \\ \sigma_{xz} \end{Bmatrix}^L = \begin{bmatrix} Q_{11} & Q_{12} & Q_{13} & O & O \\ & Q_{22} & Q_{23} & O & O \\ & & Q_{33} & O & O \\ & & & Q_{44} & Q_{45} \\ & \text{Sym} & & & Q_{55} \end{bmatrix} \begin{Bmatrix} \epsilon_x \\ \epsilon_y \\ \gamma_{xy} \\ \gamma_{yz} \\ \gamma_{xz} \end{Bmatrix}^L$$

or, in concise form, $\sigma = Q \epsilon$ \hfill (2.6)

The coefficients of the Q matrix are given by :

$$Q_{11} = C_{11} c^4 + (2C_{12}+4C_{33}) s^2 c^2 + C_{22} s^4$$

$$Q_{12} = C_{12} (s^2 + c^2) + (C_{11}-C_{22}-4C_{33}) s2 c^2$$

$$Q_{13} = (C_{11}-C_{12}-2C_{33}) c^3 s + (C_{12}-C_{22}+2C_{33}) s^3 c$$

$$Q_{22} = C_{11} s^4 + C_{22} c^4 + (2C_{12} + 4C_{33}) s^2 c^2$$

$$Q_{23} = (C_{11}-C_{12}-2C_{33}) s^3 c + (C_{12}-C_{22}+2C_{33}) s c^3$$

$$Q_{33} = (C_{11}-2C_{12}+C_{22}-2C_{33}) s^2 c^2 + C_{33}(c^4 + s^4)$$

$$Q_{44} = C_{44} c^2 + C_{55} s^2$$

$$Q_{45} = (C_{55} - C_{44}) s c$$

$$Q_{55} = C_{44} s^2 + C_{55} c^2$$

and $\quad Q_{ij} = Q_{ji}$, $\quad i,j = 1$ to 5 $\hspace{2cm}$ (2.7)

where α stands for the orientation of the lamina principal axes with respect to the laminate reference axes, as indicated in Figure 2.1.

2.5 Strain-Displacement Relationships

The definition of strains as per the theory of elasticity is adopted in obtaining the strain-displacement relations. The displacements defined by Eqns. (2.2a) and (2.2b) respectively for unsymmetric and symmetric laminates are substituted in the strain definition to yield the relations :

for symmetric laminates :

$$\epsilon_x = \frac{\partial u}{\partial x} = z\, K_x + z^3\, K_x^{*}$$

$$\epsilon_y = \frac{\partial v}{\partial y} = z\, K_y + z^3\, K_y^{*}$$

$$\gamma_{xy} = \frac{\partial u}{\partial y} + \frac{\partial v}{\partial x} = z\, K_{xy} + z^3\, K_{xy}^{*}$$

$$\gamma_{yz} = \frac{\partial v}{\partial z} + \frac{\partial w}{\partial y} = \phi_y + z^2\, \phi_y^{*}$$

$$\gamma_{xz} = \frac{\partial u}{\partial z} + \frac{\partial w}{\partial x} = \phi_x + z^2\, \phi_x^{*} \tag{2.8a}$$

where,

$$(K_x,\ K_y,\ K_{xy}) = (\frac{\partial \Theta_x}{\partial x}\ ,\ \frac{\partial \Theta_y}{\partial y}\ ,\ \frac{\partial \Theta_x}{\partial y} + \frac{\partial \Theta_y}{\partial x})$$

$$(K_x^{*},\ K_y^{*},\ K_{xy}^{*}) = (\frac{\partial \Theta_x^{*}}{\partial x}\ ,\ \frac{\partial \Theta_y^{*}}{\partial y}\ ,\ \frac{\partial \Theta_x^{*}}{\partial y} + \frac{\partial \Theta_y^{*}}{\partial x})$$

$$(\phi_x,\ \phi_y,\ \phi_x^{*},\ \phi_y^{*}) = (\Theta_x + \frac{\partial w_o}{\partial x},\ \Theta_y + \frac{\partial w_o}{\partial y},\ 3\Theta_x^{*},\ 3\Theta_y^{*}) \tag{2.8b}$$

In concise form, the flexural and transverse shear strains for any layer can be separately written using matrix notations as,

$$\epsilon_b = \begin{Bmatrix} \epsilon_x \\ \epsilon_y \\ \gamma_{xy} \end{Bmatrix} = z \begin{Bmatrix} K_x \\ K_y \\ K_{xy} \end{Bmatrix} + z^3 \begin{Bmatrix} K_x^{*} \\ K_y^{*} \\ K_{xy}^{*} \end{Bmatrix} = zK + z^3 K^{*} \tag{2.9a}$$

$$\epsilon_s = \begin{Bmatrix} \gamma_{yz} \\ \gamma_{xz} \end{Bmatrix} = \begin{Bmatrix} \emptyset_y \\ \emptyset_x \end{Bmatrix} + z^2 \begin{Bmatrix} \emptyset_y{}^* \\ \emptyset_x{}^* \end{Bmatrix} = \emptyset + z^2 \emptyset^*$$

(2.9b)

for unsymmetric laminates :

$$\epsilon_x = \frac{\partial u}{\partial x} = \epsilon_{x_o} + z K_x + z^2 \epsilon_{x_o}{}^* + z^3 K_x{}^*$$

$$\epsilon_y = \frac{\partial v}{\partial y} = \epsilon_{y_o} + z K_y + z^2 \epsilon_{y_o}{}^* + z^3 K_y{}^*$$

$$\gamma_{xy} = \frac{\partial u}{\partial y} + \frac{\partial v}{\partial x} = \epsilon_{xy_o} + z K_{xy} + z^2 \epsilon_{xy_o}{}^* + z^3 K_{xy}{}^*$$

$$\gamma_{yz} = \frac{\partial v}{\partial z} + \frac{\partial w}{\partial y} = \emptyset_y + z \psi_y + z^2 \emptyset_y{}^*$$

$$\gamma_{xz} = \frac{\partial u}{\partial z} + \frac{\partial w}{\partial x} = \emptyset_x + z \psi_x + z^2 \emptyset_x{}^*$$

(2.10a)

Some of the above components are already defined in Eqns. (2.8b). The other components are defined now as :

$$(\epsilon_{x_o}{}^*, \ \epsilon_{y_o}{}^*, \ \epsilon_{xy_o}{}^*) = (\frac{\partial u_o{}^*}{\partial x}, \ \frac{\partial v_o{}^*}{\partial y}, \ \frac{\partial u_o{}^*}{\partial y} + \frac{\partial v_o{}^*}{\partial x})$$

and $(\psi_x, \ \psi_y) = (2u_o{}^*, \ 2v_o{}^*)$

(2.10b)

The expressions for strain in any layer given by Eqns. (2.10a) can be represented in concise matrix form as,

$$\epsilon_b = \begin{Bmatrix} \epsilon_x \\ \epsilon_y \\ \gamma_{xy} \end{Bmatrix} = \begin{Bmatrix} \epsilon_{x_0} \\ \epsilon_{y_0} \\ \epsilon_{xy_0} \end{Bmatrix} + z \begin{Bmatrix} K_x \\ K_y \\ K_{xy} \end{Bmatrix} + z^2 \begin{Bmatrix} \epsilon_{x_0}^* \\ \epsilon_{y_0}^* \\ \epsilon_{xy_0}^* \end{Bmatrix}$$

$$= \epsilon_0 + z K + z^2 \epsilon_0^* + z^3 K^* \tag{2.11a}$$

$$\epsilon_s = \begin{Bmatrix} \gamma_{yz} \\ \gamma_{xz} \end{Bmatrix} = \begin{Bmatrix} \phi_y \\ \phi_x \end{Bmatrix} + z \begin{Bmatrix} \psi_y \\ \psi_x \end{Bmatrix} + z^2 \begin{Bmatrix} \phi_y^* \\ \phi_x^* \end{Bmatrix}$$

$$= \phi + z \psi + z^2 \phi^* \tag{2.11b}$$

2.6 Laminate Constitutive Relations

The strain energy of the plate, which is basically
defined in terms of physical stress and strain components
can be conveniently written in terms of stress resultants
and strains. The stress resultants so used are nothing but
the integral of the physical stress components through the
thickness of the plate. These stress resultants for the
differential element of a laminate are expressed in terms
of midplane plate curvatures and shear rotations, which are
a function of the assumed displacement field.

The strain energy 'U' for the plate with volume 'V' and
surface area 'A' can be written as

$$U = \frac{1}{2} \int_V \epsilon^{\mathrm{T}} \sigma \, dv \qquad (2.12)$$

Writing in terms of the individual stress components,

$$U = \frac{1}{2} \int_V [\epsilon_x \sigma_x + \epsilon_y \sigma_y + \gamma_{xy} \sigma_{xy} + \gamma_{xz} \sigma_{xz} + \gamma_{yz} \sigma_{yz}] \, dv \qquad (2.13)$$

Substituting the expressions for the strain components given by (2.8a) and (2.10a), and conducting explicit integration through the laminate thickness, the strain energy is obtained in terms of stress resultants, i.e.,

$$U = \frac{1}{2} \int_A \bar{\epsilon}^{\,T} \bar{\sigma} \, dA \qquad (2.14)$$

where $\bar{\epsilon}$ and $\bar{\sigma}$ are defined as,

for symmetric laminates :

$$\bar{\epsilon} = (K_x, K_y, K_{xy}, K_x^*, K_y^*, K_{xy}^*, \emptyset_y, \emptyset_x, \emptyset_y^*, \emptyset_x^*)$$

$$= (K, K^*, \emptyset, \emptyset^*) \qquad (2.15a)$$

$$\bar{\sigma} = (M_x, M_y, M_{xy}, M_x^*, M_y^*, M_{xy}^*, S_y, S_x, S_y^*, S_x^*)$$

$$= (M, M^*, S, S^*) \qquad (2.15b)$$

for unsymmetric laminates :

$$\bar{\epsilon} = (\epsilon_{x_o}, \epsilon_{y_o}, \epsilon_{xy_o}, \epsilon_{x_o}^*, \epsilon_{y_o}^*, \epsilon_{xy_o}^*, K_x, K_y, K_{xy}, K_x^*, K_y^*$$

$$K_{xy}^*, \phi_y, \phi_x, \psi_y, \psi_x, \phi_y^*, \phi_x^*)$$

$$= (\epsilon_o, \epsilon_o^*, K, K^*, \phi, \psi, \phi^*) \qquad (2.16a)$$

$$\bar{\sigma} = (N_x, N_y, N_{xy}, N_x^*, N_y^*, N_{xy}^*, M_x, M_y, M_{xy},$$

$$M_x^*, M_y^*, M_{xy}^*, S_y, S_x, T_y, T_x, S_y^*, S_x^*)$$

$$= (N, N^*, M, M^*, S, T, S^*) \qquad (2.16b)$$

where, the components of the stress resultant vector $\bar{\sigma}$ are defined by

$$(N_x, N_y, N_{xy}) = \sum_{L=1}^{N_L} \int_{h_L}^{h_{L+1}} (\sigma_x, \sigma_y, \sigma_{xy})^L \, dz$$

$$(M_x, M_y, M_{xy}) = \sum_{L=1}^{NL} \int_{h_L}^{h_{L+1}} (\sigma_x, \sigma_y, \sigma_{xy})^L \, zdz$$

$$(N_x^*, N_y^*, N_{xy}^*) = \sum_{L=1}^{NL} \int_{h_L}^{h_{L+1}} (\sigma_x, \sigma_y, \sigma_{xy})^L \, z^2dz$$

$$(M_x^*, M_y^*, M_{xy}^*) = \sum_{L=1}^{NL} \int_{h_L}^{h_{L+1}} (\sigma_x, \sigma_y, \sigma_{xy})^L \, z^3dz$$

$$(S_x, S_y) = \sum_{L=1}^{NL} \int_{h_L}^{h_{L+1}} (\sigma_{xz}, \sigma_{yz})^L \, dz$$

$$(T_x, T_y) = \sum_{L=1}^{NL} \int_{h_L}^{h_{L+1}} (\sigma_{xz}, \sigma_{yz})^L \, z\,dz$$

$$(S_x^*, S_y^*) = \sum_{L=1}^{NL} \int_{h_L}^{h_{L+1}} (\sigma_{xz}, \sigma_{yz})^L \, z^2 dz \qquad (2.17)$$

The stresses are now written in terms of the generalized strain components given by (2.15a) and (2.16a). This is accomplished by substituting strain expressions given by (2.9) and (2.11) in the expressions (2.6) for the stresses. Thus, the stresses in the Lth layer are given by the following relations :

for symmetric laminates :

$$\left\{ \begin{matrix} \sigma_x \\ \sigma_y \\ \sigma_{xy} \end{matrix} \right\}^L = \left[\bar{Q} \right]^L z \left\{ \begin{matrix} K_x \\ K_y \\ K_{xy} \end{matrix} \right\} + \left[\bar{Q} \right]^L z^3 \left\{ \begin{matrix} K_x^* \\ K_y^* \\ K_{xy}^* \end{matrix} \right\}$$

$$\left\{ \begin{matrix} \sigma_{yz} \\ \sigma_{xz} \end{matrix} \right\}^L = \begin{bmatrix} Q_{44} & Q_{45} \\ Q_{45} & Q_{55} \end{bmatrix}^L \left\{ \begin{matrix} \phi_y \\ \phi_x \end{matrix} \right\} + \begin{bmatrix} Q_{44} & Q_{45} \\ Q_{45} & Q_{55} \end{bmatrix}^L z^2 \left\{ \begin{matrix} \phi_y^* \\ \phi_x^* \end{matrix} \right\}$$

$$(2.18)$$

for unsymmetric laminates :

$$
\begin{Bmatrix} \sigma_x \\ \sigma_y \\ \sigma_{xy} \end{Bmatrix}^L = \left[\overline{Q}\right]^L \begin{Bmatrix} \epsilon_{x_o} \\ \epsilon_{y_o} \\ \epsilon_{xy_o} \end{Bmatrix} + \left[\overline{Q}\right]^L z \begin{Bmatrix} K_x \\ K_y \\ K_{xy} \end{Bmatrix}
$$

$$
+ \left[\overline{Q}\right]^L z^2 \begin{Bmatrix} \epsilon_{x_o}^* \\ \epsilon_{y_o}^* \\ \epsilon_{xy_o}^* \end{Bmatrix} + \left[\overline{Q}\right]^L z^3 \begin{Bmatrix} K_x^* \\ K_y^* \\ K_{xy}^* \end{Bmatrix}
$$

$$
\begin{Bmatrix} \sigma_{yz} \\ \sigma_{xz} \end{Bmatrix}^L = \begin{bmatrix} Q_{44} & Q_{45} \\ Q_{45} & Q_{55} \end{bmatrix}^L \begin{Bmatrix} \phi_y \\ \phi_x \end{Bmatrix} + \begin{bmatrix} Q_{44} & Q_{45} \\ Q_{45} & Q_{55} \end{bmatrix}^L z \begin{Bmatrix} \psi_y \\ \psi_x \end{Bmatrix}
$$

$$
+ \begin{bmatrix} Q_{44} & Q_{45} \\ Q_{45} & Q_{55} \end{bmatrix} z^2 \begin{Bmatrix} \phi_y^* \\ \phi_x^* \end{Bmatrix} \tag{2.19}
$$

where

$$
\left[\overline{Q}\right]^L = \begin{bmatrix} Q_{11} & Q_{12} & Q_{13} \\ & Q_{22} & Q_{23} \\ \text{Sym} & & Q_{33} \end{bmatrix}^L \tag{2.20}
$$

These expressions for stresses, when substituted in expressions (2.17) yield the laminate constitute relations, which relate the stress resultants to the generalized strains, as follows :

$$
\begin{Bmatrix}
N_x \\
N_y \\
N_{xy} \\
N_x^* \\
N_y^* \\
N_{xy}^* \\
M_x \\
M_y \\
M_{xy} \\
M_x^* \\
M_y^* \\
M_{xy}^*
\end{Bmatrix}
=
\sum_{L=1}^{NL}
\begin{bmatrix}
[\bar{Q}]H_1 & [\bar{Q}]H_3 & [\bar{Q}]H_2 & [\bar{Q}]H_4 \\
 & [\bar{Q}]H_5 & [\bar{Q}]H_4 & [\bar{Q}]H_6 \\
 & & [\bar{Q}]H_3 & [\bar{Q}]H_5 \\
\text{Symmetric} & & & [\bar{Q}]H_7
\end{bmatrix}
\begin{Bmatrix}
\epsilon_{x_o} \\
\epsilon_{y_o} \\
\epsilon_{xy_o} \\
\epsilon_{x_o}^* \\
\epsilon_{y_o}^* \\
\epsilon_{xy_o}^* \\
K_x \\
K_y \\
K_{xy} \\
K_x^* \\
K_y^* \\
K_{xy}^*
\end{Bmatrix}
$$

$$(2.21a)$$

$$
\begin{Bmatrix}
S_y \\
S_x \\
T_y \\
T_x \\
S_y^* \\
S_x^*
\end{Bmatrix}
=
\sum_{L=1}^{NL}
\begin{bmatrix}
Q_{44}H_1 & Q_{45}H_1 & Q_{44}H_2 & Q_{45}H_2 & Q_{44}H_3 & Q_{45}H_3 \\
 & Q_{55}H_1 & Q_{45}H_2 & Q_{55}H_2 & Q_{45}H_3 & Q_{55}H_3 \\
 & & Q_{44}H_3 & Q_{45}H_3 & Q_{44}H_4 & Q_{45}H_4 \\
 & & & Q_{55}H_3 & Q_{45}H_4 & Q_{55}H_4 \\
 & & & & Q_{44}H_5 & Q_{45}H_5 \\
 & & & & & Q_{55}H_5
\end{bmatrix}
\begin{Bmatrix}
\phi_y \\
\phi_x \\
\psi_y \\
\psi_x \\
\phi_y^* \\
\phi_x^*
\end{Bmatrix}
$$

$$(2.21b)$$

where, $H_i = \frac{1}{i}(h_{L+1}^i - h_L^i)$, $\quad i = 1,2,3, \ldots 7$

The relations (2.21a) and (2.21b) can be represented together in a concise matrix form as follows :

$$
\begin{Bmatrix} N \\ N^* \\ M \\ M^* \\ S \\ T \\ S^* \end{Bmatrix} = \begin{bmatrix} D_m & D_c & O \\ D_c^{\ T} & D_b & O \\ O & O & D_s \end{bmatrix} \begin{Bmatrix} \varepsilon_o \\ \varepsilon_o^* \\ K \\ K^* \\ \phi \\ \psi \\ \phi^* \end{Bmatrix}
$$

(2.22a)

or, $\quad \bar{\sigma} = D\,\bar{\varepsilon}$

(2.22b)

Similarly, for the particular case of the symmetric laminates, the relations (2.21) reduce to the form as given below, where the coupling terms vanish.

$$
\begin{Bmatrix} M_x \\ M_y \\ M_{xy} \\ M_x^* \\ M_y^* \\ M_{xy}^* \end{Bmatrix} = \begin{bmatrix} [\bar{Q}]\,H_3 & [\bar{Q}]\,H_5 \\ & \\ \text{Sym.} & [\bar{Q}]\,H_7 \end{bmatrix} \begin{Bmatrix} K_x \\ K_y \\ K_{xy} \\ K_x^* \\ K_y^* \\ K_{xy}^* \end{Bmatrix}
$$

(2.23a)

$$
\begin{Bmatrix} S_y \\ S_x \\ S_y^* \\ S_x^* \end{Bmatrix} = \begin{bmatrix} Q_{44}H_1 & Q_{45}H_1 & Q_{44}H_3 & Q_{45}H_3 \\ & Q_{55}H_1 & Q_{45}H_3 & Q_{55}H_3 \\ & & Q_{44}H_5 & Q_{45}H_5 \\ \text{Sym.} & & & Q_{55}H_5 \end{bmatrix} \begin{Bmatrix} \phi_y \\ \phi_x \\ \phi_y^* \\ \phi_x^* \end{Bmatrix}
$$

(2.23b)

2.7 Interlaminar Stresses Using Equilibrium Equations

The stress-strain constitutive relations of the form (2.18) and (2.19) are generally used for the evaluation of interlaminar shear-stresses (σ_{xz}, σ_{yz}). The present theory leads to realistic parabolic transverse shear stress distribution through the laminate thickness. But, when the constitutive relations (2.18) and (2.19) are used, they lead to the discontinuity of interlaminar stresses at the interface of two adjacent lamina with non-identical Q matrices. This violates the equilibrium conditions. In the present section, an alternative approach is adopted for the determination of σ_{xz} and σ_{yz}. The equilibrium equations of elasticity for each layer are used to derive expressions for the interlaminar shear stresses. The expressions for inplane stresses from constitutive relations are utilised.

We have, for each layer,

$$\frac{\partial \sigma_x}{\partial x} + \frac{\partial \sigma_{xy}}{\partial y} + \frac{\partial \sigma_{xz}}{\partial z} = 0 \qquad (2.24a)$$

$$\frac{\partial \sigma_{xy}}{\partial x} + \frac{\partial \sigma_y}{\partial y} + \frac{\partial \sigma_{yz}}{\partial z} = 0 \qquad (2.24b)$$

In an alternate form,

$$\sigma_{xz}^{L}\bigg|_{z=h_{L+1}} = -\sum_{i=1}^{L} \int_{h_i}^{h_{i+1}} \left(\frac{\partial \sigma_x^i}{\partial x} + \frac{\partial \sigma_{xy}^i}{\partial y}\right) dz \qquad (2.25a)$$

$$\sigma_{yz}^{L}\bigg|_{z=h_{L+1}} = -\sum_{i=1}^{L} \int_{h_i}^{h_i+1} \left(\frac{\partial \sigma_y^i}{\partial y} + \frac{\partial \sigma_{xy}^i}{\partial x}\right) dz \qquad (2.25b)$$

The expressions for the inplane stresses given by (2.18) and (2.19) are substituted in the above and integration is performed through the thickness of the layer. This yields the following expressions :

for symmetric laminates :

$$\sigma_{xz}^{L}\bigg|_{z=h_{L+1}} = -\sum_{i=1}^{L} \left[Q_{11}^{i}\left(H_2 \frac{\partial^2 \Theta_x}{\partial x^2} + H_4 \frac{\partial^2 \Theta_x^*}{\partial x^2}\right) \right.$$

$$+ Q_{12}^{i}\left(H_2 \frac{\partial^2 \Theta_y}{\partial x \partial y} + H_4 \frac{\partial^2 \Theta_y^*}{\partial x \partial y}\right)$$

$$+ Q_{13}^{i}\left(2H_2 \frac{\partial^2 \Theta_x}{\partial x \partial y} + H_2 \frac{\partial^2 \Theta_y}{\partial x^2} + 2H_4 \frac{\partial^2 \Theta_x^*}{\partial x \partial y} + H_4 \frac{\partial^2 \Theta_y^*}{\partial x^2}\right)$$

$$+ Q_{23}^{i}\left(H_2 \frac{\partial^2 \Theta_y}{\partial y^2} + H_4 \frac{\partial^2 \Theta_y^*}{\partial y^2}\right)$$

$$+ Q_{33}^i (H_2 \frac{\partial^2 \Theta_x}{\partial y^2} + H_2 \frac{\partial^2 \Theta_y}{\partial x \partial y} + H_4 \frac{\partial^2 \Theta_x^*}{\partial y^2} + H_4 \frac{\partial^2 \Theta_y^*}{\partial x \partial y})]$$

$$(2.26a)$$

$$\sigma_{yz}^L \Big|_{z=h_L+1} = - \sum_{i=1}^{L} [Q_{12}^i (H_2 \frac{\partial^2 \Theta_x}{\partial x \partial y} + H_4 \frac{\partial^2 \Theta_x^*}{\partial x \partial y})$$

$$+ Q_{22}^i (H_2 \frac{\partial^2 \Theta_y}{\partial y^2} + H_4 \frac{\partial^2 \Theta_y^*}{\partial y^2})$$

$$+ Q_{23}^i (H_2 \frac{\partial^2 \Theta_x}{\partial y^2} + 2H_2 \frac{\partial^2 \Theta_y}{\partial x \partial y} + H_4 \frac{\partial^2 \Theta_x^*}{\partial y^2} + 2H_4 \frac{\partial^2 \Theta_y^*}{\partial x \partial y})$$

$$+ Q_{13}^i (H_2 \frac{\partial^2 \Theta_x}{\partial x^2} + H_4 \frac{\partial^2 \Theta_x^*}{\partial x^2})$$

$$+ Q_{33}^i (H_2 \frac{\partial^2 \Theta_x}{\partial x \partial y} + H_2 \frac{\partial^2 \Theta_y}{\partial x \partial y} + H_4 \frac{\partial^2 \Theta_x^*}{\partial x \partial y} + H_4 \frac{\partial^2 \Theta_y^*}{\partial x^2})]$$

$$(2.26b)$$

For unsymmetric laminates :

$$\sigma_{xz}^L \Big|_{z=h_{L+1}} = - \sum_{i=1}^{L} [Q_{11}^i (H_1 \frac{\partial^2 u_o}{\partial x^2} + H_2 \frac{\partial^2 \Theta_x}{\partial x^2} + H_3 \frac{\partial^2 u_o^*}{\partial x^2}$$

$$+ H_4 \frac{\partial^2 \Theta_x^*}{\partial x^2})$$

$$+ Q_{12}^i (H_1 \frac{\partial^2 v_o}{\partial x \partial y} + H_2 \frac{\partial^2 \Theta_y}{\partial x \partial y} + H_3 \frac{\partial^2 v_o^*}{\partial x \partial y} + H_4 \frac{\partial^2 \Theta_y^*}{\partial x \partial y})$$

$$+ Q_{13}^i (2H_1 \frac{\partial^2 u_o}{\partial x \partial y} + 2H_2 \frac{\partial^2 \Theta_x}{\partial x \partial y} + 2H_3 \frac{\partial^2 uo^*}{\partial x \partial y} + 2H_4 \frac{\partial^2 \Theta_x^*}{\partial x \partial y}$$

$$+ H_1 \frac{\partial^2 v_o}{\partial x^2} + H_2 \frac{\partial^2 \Theta_y}{\partial x^2} + H_3 \frac{\partial^2 v_o^*}{\partial x^2} + H_4 \frac{\partial^2 \Theta_y^*}{\partial x^2})$$

$$+ Q_{33}^i (H_1 \frac{\partial^2 u_o}{\partial y^2} + H_2 \frac{\partial^2 \Theta_y}{\partial y^2} + H_3 \frac{\partial^2 v_o^*}{\partial y^2} + H_4 \frac{\partial^2 \Theta_y^*}{\partial y^2})$$

$$+ Q_{33}^i (H_1 \frac{\partial^2 u_o}{\partial y^2} + H_2 \frac{\partial^2 \Theta_x}{\partial y^2} + H_3 \frac{\partial^2 u_o^*}{\partial y^2} + H_4 \frac{\partial^2 \Theta_x^*}{\partial y^2}$$

$$+ H_1 \frac{\partial^2 v_o}{\partial x \partial y} + H_2 \frac{\partial^2 \Theta_y}{\partial x \partial y} + H_3 \frac{\partial^2 v_o^*}{\partial x \partial y} + H_4 \frac{\partial^2 \Theta_y^*}{\partial x \partial y})] \qquad (2.27a)$$

$$\sigma_{yz}^L \Big|_{z=h_{L+1}} = \sum_{i=1}^{L} [Q_{12}^i (H_1 \frac{\partial^2 u_o}{\partial x \partial y} + H_2 \frac{\partial^2 \Theta_x}{\partial x \partial y} + H_3 \frac{\partial^2 u_o^*}{\partial x \partial y} + H_4 \frac{\partial^2 \Theta_x^*}{\partial x \partial y})$$

$$+ Q_{22}^i (H_1 \frac{\partial^2 v_o}{\partial y^2} + H_2 \frac{\partial^2 \Theta_y}{\partial y^2} + H_3 \frac{\partial^2 v_o^*}{\partial y^2} + H_4 \frac{\partial^2 \Theta_y^*}{\partial y^2})$$

$$+ Q_{23}^i (H_1 \frac{\partial^2 u_o}{\partial y^2} + H_2 \frac{\partial^2 \Theta_x}{\partial y^2} + H_3 \frac{\partial^2 u_o^*}{\partial y^2} + H_4 \frac{\partial^2 \Theta_x^*}{\partial y^2}$$

$$+ 2H_1 \frac{\partial^2 v_o}{\partial x \partial y} + 2H_2 \frac{\partial^2 \Theta_y}{\partial x \partial y} + 2H_3 \frac{\partial^2 v_o^*}{\partial x \partial y} + 2H_4 \frac{\partial^2 \Theta_y^*}{\partial x \partial y})$$

$$+ Q_{13}^i (H_1 \frac{\partial^2 u_o}{\partial x^2} + H_2 \frac{\partial^2 \Theta_x}{\partial x^2} + H_3 \frac{\partial^2 u_o^*}{\partial x^2} + H_4 \frac{\partial^2 \Theta_x^*}{\partial x^2})$$

$$+ Q_{33}^i (H_1 \frac{\partial^2 u_o}{\partial x \partial y} + H_2 \frac{\partial^2 \Theta_x}{\partial x \partial y} + H_3 \frac{\partial^2 u_o^*}{\partial x \partial y} + H_4 \frac{\partial^2 \Theta_x^*}{\partial x \partial y}$$

$$+ H_1 \frac{\partial^2 v_o}{\partial x^2} + H_2 \frac{\partial^2 \Theta_y}{\partial x^2} + H_3 \frac{\partial^2 v_o^*}{\partial x^2} + H_4 \frac{\partial^2 \Theta_y^*}{\partial x^2})] \qquad (2.27b)$$

CHAPTER 3

FINITE ELEMENT DISCRETIZATION

3.1 Preliminary Remarks

The finite element displacement formulation is used for obtaining the solutions for the fundamental equations derived in the second chapter. The continuum is separated by imaginary lines into a number of finite elements. A set of functions is chosen to define the state of displacements over each element in terms of its nodal displacements. The total potential of the system is then written in terms of the prescribed displacement field and the principle of minimum potential energy is applied to yield the equilibrium equations.

3.2 Element Shape Functions

The domain can be discretized into 'NEL' number of elements and the total potential (π) of the structure be written as a summation of the total potential of individual elements (π^e), i.e.,

$$\pi = \sum_{e=1}^{NEL} \pi^e \qquad\qquad (3.1)$$

In the displacement based formulation, π^e is written as a function of unknown displacement variables defined by assumed displacement models. For the displacement models given by Eqns. (2.2a) and (2.2b) respectively for unsymmetric and symmetric cases, the vector of unknown displacement variables can be written as,

Symmetric : $\delta = (w_o, \Theta_x, \Theta_y, \Theta_x^*, \Theta_y^*)^T$ (3.2)

Unsymmetric : $\delta = (u_o, v_o, w_o, \Theta_x, \Theta_y, u_o^*, v_o^*, \Theta_x^*, \Theta_y^*)^T$ (3.3)

The variation of these over the element is defined in terms of normalized coordinates ξ and η, by isoparametric shape (interpolating) functions, such that,

$$\delta = \sum_{i=1}^{NN} N_i \ \delta_i$$ (3.4)

where, NN denotes the number of nodes per element, N_i is the shape function associated with node i, and δ_i is the generalized displacement vector corresponding to the ith node. In the present formulation all the components of the generalized displacement vector of an element δ, are defined by identical shape functions. The nine-noded lagrangian quadratic plate element is adopted which accounts for parabolic variation of the displacements over the element. The shape functions are given by,

for corner nodes :

$$N_i^e = \frac{1}{4}(1 + \xi\xi_i)(1 + \eta\eta_i)\,\xi\xi_i\,\eta\eta_i \qquad (3.5a)$$

for midside nodes :

$$N_i^e = \frac{1}{2}\,\xi\xi_i(1 + \xi\xi_i)(1 - \eta^2) + \frac{1}{2}\,\eta\eta_i(1 + \eta\eta_i)(1 - \xi^2) \quad (3.5b)$$

for the central node

$$N_9 = (1 - \xi^2)(1 - \eta^2) \qquad (3.5c)$$

By definition, the shape functions for an isoparametric element are used to define the coordinates at any point on the reference x-y plane of the plate, viz.,

$$x = \sum_{i=1}^{NN} N_i x_i, \qquad y = \sum_{i=1}^{NN} N_i y_i \qquad (3.6)$$

3.3 Element Stiffness Matrix

The stiffness matrix is obtained by expressing the internal strain energy for an element in terms of the unknown nodal displacements. The strain energy is contributed by membrane, flexure and shear strains, the membrane strains being absent for the particular case of symmetric laminates.

The membrane strains, bending curvature and shear strains are written in a matrix form in terms of the nodal displacements using the Equations (2.8b) and (2.10b), as given below :

$$\left\{ \begin{array}{c} \epsilon_o \\ \\ \epsilon_o^* \end{array} \right\} = L_m \, \delta \qquad \left\{ \begin{array}{c} K \\ \\ K^* \end{array} \right\} = L_b \, \delta \qquad \left\{ \begin{array}{c} \emptyset \\ \psi \\ \emptyset^* \end{array} \right\} = L_s \, \delta \qquad (3.7)$$

For symmetric laminates ϵ_o, ϵ_o^* and ψ do not exist. All the vectors and matrices L_b, L_s and L_m in relation (3.7) are described below :

for symmetric laminates :

$$\delta = (w_o, \Theta_x, \Theta_y, \Theta_x^*, \Theta_y^*)^T \qquad (3.8a)$$

$$(K^T, K^{*T}) = (K_x, K_y, K_{xy}, K_x^*, K_y^*, K_{xy}^*) \qquad (3.8b)$$

$$(\emptyset^T, \emptyset^{*T}) = (\emptyset_x, \emptyset_y, \emptyset_x^*, \emptyset_y^*) \qquad (3.8c)$$

$$L_b = \begin{bmatrix} 0 & \partial/\partial x & 0 & 0 & 0 \\ 0 & 0 & \partial/\partial y & 0 & 0 \\ 0 & \partial/\partial y & \partial/\partial x & 0 & 0 \\ 0 & 0 & 0 & \partial/\partial x & 0 \\ 0 & 0 & 0 & 0 & \partial/\partial y \\ 0 & 0 & 0 & \partial/\partial y & \partial/\partial x \end{bmatrix} \qquad (3.8d)$$

$$L_s = \begin{bmatrix} \partial/\partial x & 1 & 0 & 0 & 0 \\ \partial/\partial y & 0 & 1 & 0 & 0 \\ 0 & 0 & 0 & 3 & 0 \\ 0 & 0 & 0 & 0 & 3 \end{bmatrix} \qquad (3.8e)$$

for unsymmetric laminates :

$$\delta = (u_o, v_o, w_o, \Theta_x, \Theta_y, u_o^*, v_o^*, \Theta_x^*, \Theta_y^*)^T \qquad (3.9a)$$

$$(\epsilon_o^T, \epsilon_o^*)^T) = (\epsilon_{x_o}, \epsilon_{y_o}, \epsilon_{xy_o}, \epsilon_{x_o}^*, \epsilon_{y_o}^*, \epsilon_{xy_o}^*) \qquad (3.9b)$$

$$(K^T, K^{*T}) = (K_x, K_y, K_{xy}, K_x^*, K_y^*, K_{xy}^*) \qquad (3.9c)$$

$$(\phi^T, \psi^T, \phi^{*T}) = (\phi_x, \phi_y, \psi_x, \psi_y, \phi_x^*, \phi_y^*) \qquad (3.9d)$$

$$L_m = \begin{bmatrix} \dfrac{\partial}{\partial x} & 0 & 0 & 0 & 0 & 0 & 0 & 0 & 0 \\ 0 & \dfrac{\partial}{\partial y} & 0 & 0 & 0 & 0 & 0 & 0 & 0 \\ \dfrac{\partial}{\partial y} & \dfrac{\partial}{\partial x} & 0 & 0 & 0 & 0 & 0 & 0 & 0 \\ 0 & 0 & 0 & 0 & 0 & \dfrac{\partial}{\partial x} & 0 & 0 & 0 \\ 0 & 0 & 0 & 0 & 0 & 0 & \dfrac{\partial}{\partial y} & 0 & 0 \\ 0 & 0 & 0 & 0 & 0 & \dfrac{\partial}{\partial y} & \dfrac{\partial}{\partial x} & 0 & 0 \end{bmatrix}$$

$$(3.9e)$$

$$
L_b = \begin{bmatrix}
0 & 0 & 0 & \partial/\partial x & 0 & 0 & 0 & 0 & 0 \\
0 & 0 & 0 & 0 & \partial/\partial y & 0 & 0 & 0 & 0 \\
0 & 0 & 0 & \partial/\partial y & \partial/\partial x & 0 & 0 & 0 & 0 \\
0 & 0 & 0 & 0 & 0 & 0 & 0 & \partial/\partial x & 0 \\
0 & 0 & 0 & 0 & 0 & 0 & 0 & 0 & \partial/\partial y \\
0 & 0 & 0 & 0 & 0 & 0 & 0 & \partial/\partial y & \partial/\partial x
\end{bmatrix}
$$

(3.9f)

$$
L_s = \begin{bmatrix}
0 & 0 & \partial/\partial x & 1 & 0 & 0 & 0 & 0 & 0 \\
0 & 0 & \partial/\partial y & 0 & 1 & 0 & 0 & 0 & 0 \\
0 & 0 & 0 & 0 & 0 & 2 & 0 & 0 & 0 \\
0 & 0 & 0 & 0 & 0 & 0 & 2 & 0 & 0 \\
0 & 0 & 0 & 0 & 0 & 0 & 0 & 3 & 0 \\
0 & 0 & 0 & 0 & 0 & 0 & 0 & 0 & 3
\end{bmatrix}
$$

(3.9g)

The generalized displacement vector is defined in terms of its nodal values in relation (3.4) using interpolating functions. Using this relation, along with the expressions for strains in matrix form given by relation (3.7), the generalized strain vector can be expressed in terms of nodal displacement values as,

$$
\begin{Bmatrix} \epsilon_o \\ \epsilon_o^* \end{Bmatrix} = L_m \, \delta = L_m \sum_{i=1}^{NN} N_i \, \delta_i = \sum_{i=1}^{NN} Bm_i \, \delta_i = Bm \, d
$$

$$\begin{Bmatrix} K \\ \\ K^* \end{Bmatrix} = L_b \, \delta = L_b \sum_{i=1}^{NN} N_i \, \delta_i = \sum_{i=1}^{NN} B_{b_i} \, \delta_i = B_b \, d$$

$$\begin{Bmatrix} \phi \\ \\ \psi \\ \\ \phi^* \end{Bmatrix} = L_s \, \delta = L_s \sum_{i=1}^{NN} N_i \, \delta_i = \sum_{i=1}^{NN} B_{s_i} \, \delta_i = B_s \, d \qquad (3.10a)$$

where, $B_{m_i} = L_m \, N_i$, $B_{b_i} = L_b \, N_i$, $B_{s_i} = L_s \, N_i$ \qquad (3.10b)

and

$$B_m = [B_{m_1} \quad B_{m_2} \quad \cdots \quad B_{m_{NN}}]$$

$$B_b = [B_{b_1} \quad B_{b_2} \quad \cdots \quad B_{b_{NN}}]$$

$$B_s = [B_{s_1} \quad B_{s_2} \quad \cdots \quad B_{s_{NN}}] \qquad (3.10c)$$

and

$$d^T = (\delta_1^{\,T}, \, \delta_2^{\,T}, \, \cdots \quad \delta_{NN}^T] \qquad (3.10d)$$

The internal strain energy of an element can be obtained by multiplying the stress resultants with appropriate strains and integrating them over the area of the element, i.e.,

$$U^e = \frac{1}{2} \int_A [(\Theta_o^T, \Theta_o^{*T}) \begin{Bmatrix} N \\ N^* \end{Bmatrix} + (K^T, K^{*T}) \begin{Bmatrix} M \\ M^* \end{Bmatrix}$$

$$+ (\phi^T, \psi^T, \phi^{*T}) \begin{Bmatrix} S \\ \overline{T} \\ S^* \end{Bmatrix}] \, dA \qquad (3.11)$$

The stress resultants can be substituted by midsurface strain vectors using Equations (2.22a). Thus, the expression (3.11) changes to,

$$U^e = \frac{1}{2} \int_A [(\Theta_o^T, \Theta_o^{*T}) D_m \begin{Bmatrix} \Theta_o^T \\ \Theta_o^{*T} \end{Bmatrix} + (\Theta_o^T, \Theta_o^{*T}) D_c \begin{Bmatrix} K^T \\ K^{*T} \end{Bmatrix}$$

$$+ (K^T, K^{*T}) D_c^T \begin{Bmatrix} \Theta_o^T \\ \Theta_o^{*T} \end{Bmatrix} + (K^T, K^{*T}) D_b \begin{Bmatrix} K^T \\ K^{*T} \end{Bmatrix}$$

$$+ (\phi^T, \psi^T, \phi^{*T}) D_s \begin{Bmatrix} \phi \\ \psi \\ \phi^* \end{Bmatrix}] \, dA \qquad (3.12)$$

Substituting the strain vectors by the nodal displacement vector, using Equations (3.10a),

$$U^e = \frac{1}{2} \int_A [d^T (B_m^T D_m B_m) d + d^T (B_m^T D_c B_b) d + d^T (B_b^T D_c^T B_m) d$$

$$+ d^T (B_b^T D_b B_b) d + d^T (B_s^T D_s B_s) d] \, dA \qquad (3.13)$$

or,

$$U^e = \frac{1}{2} d^T [K]^e d \qquad (3.14)$$

where

$$[K]^e = \int_A (B_m^T D_m B_m + B_m^T D_c B_b + B_b^T D_c^T B_m$$

$$+ B_b^T D_b B_b + B_s^T D_s B_s) \, dA \qquad (3.15)$$

$[K]^e$ is identified as the stiffness matrix for an element e. For symmetric laminates, the quantities in the above expression related to coupling do not exist.

3.4 Geometric Stiffness Matrix

For the stability problem, the geometric stiffness matrix is derived by considering the work done by inplane stresses σ_x, σ_y and σ_{xy}, while acting through the second order contributions from lateral displacement w to strains ϵ_x, ϵ_y and ϵ_{xy}.

These strain contributions are :

$$\epsilon_{x_{NL}} = \frac{1}{2} \left(\frac{\partial w}{\partial x}\right)^2$$

$$\epsilon_{y_{NL}} = \frac{1}{2} \left(\frac{\partial w}{\partial y}\right)^2$$

$$\epsilon_{xy_{NL}} = \frac{\partial w}{\partial x} \frac{\partial w}{\partial y} \qquad (3.16)$$

The work done by inplane stresses on an element while acting through the above strains is :

$$W_g^e = \frac{1}{2} \int_V [\sigma_x (\frac{\partial w}{\partial x})^2 + \sigma_y (\frac{\partial w}{\partial y})^2 + 2\sigma_{xy}(\frac{\partial w}{\partial x} \frac{\partial w}{\partial y})] \, dV \qquad (3.17)$$

After integrating through the thickness, the expression for work done can be written in terms of stress resultants in a convenient form as,

$$W_g^e = \frac{1}{2} \int_A [\begin{Bmatrix} \partial w/\partial x \\ \partial w/\partial y \end{Bmatrix}^T \begin{bmatrix} N_x & N_{xy} \\ N_{xy} & N_y \end{bmatrix} \begin{Bmatrix} \partial w/\partial x \\ \partial w/\partial y \end{Bmatrix}] \, dA \qquad (3.18)$$

It is well known that a 'consistent' geometric stiffness matrix yields more accurate buckling loads and mode shapes which are proven upper bounds to the exact solution.[30] In this approach, the displacement functions as used for deriving, the elastic stiffness matrix are used to build the geometric stiffness matrix.

The derivatives of w can be written in a convenient matrix form as,

$$\begin{Bmatrix} \dfrac{\partial w}{\partial x} \\ \\ \dfrac{\partial w}{\partial y} \end{Bmatrix} = L_g \, \delta \qquad (3.19)$$

δ is already defined in (3.8a) and (3.9a) respectively for symmetric and unsymmetric laminates. The matrix L_g for the two cases is written below :

for symmetric laminates :

$$L_g = \begin{bmatrix} \partial/\partial x & 0 & 0 & 0 & 0 \\ \partial/\partial y & 0 & 0 & 0 & 0 \end{bmatrix}$$ (3.20)

for unsymmetric laminates :

$$L_g = \begin{bmatrix} 0 & 0 & \partial/\partial x & 0 & 0 & 0 & 0 & 0 & 0 \\ 0 & 0 & \partial/\partial y & 0 & 0 & 0 & 0 & 0 & 0 \end{bmatrix}$$ (3.21)

The derivatives $\partial w/\partial x$ and $\partial w/\partial y$ can be expressed

in terms of nodal displacements using relation (3.4) as,

$$\begin{Bmatrix} \dfrac{\partial w}{\partial x} \\ \\ \dfrac{\partial w}{\partial y} \end{Bmatrix} = L_g \, \delta = L_g \sum_{i=1}^{NN} N_i \delta_i = \sum_{i=1}^{NN} B_{g_i} \, \delta_i = B_g \, d$$ (3.22)

where, $B_g = [B_{g_1} \quad B_{g_2} \quad \ldots \quad B_{g_{NN}}]$ and d is as

defined in (3.10d).

Substituting (3.22) in (3.18), we get,

$$W_g^e = \frac{1}{2} \int_A [d^T \, B_g^T \begin{bmatrix} N_x & N_{xy} \\ N_{xy} & N_y \end{bmatrix} B_g \, d] \, dA$$ (3.23)

or

$$W_g^e = \frac{1}{2} \, d^T \, [G]^e \, d$$ (3.24)

where,

$$G^e = \int_A \lfloor B_g^T \begin{bmatrix} N_x & N_{xy} \\ \\ N_{xy} & N_y \end{bmatrix} B_g \rfloor \, dA \qquad (3.25)$$

G^e is known as the geometric stiffness matrix corresponding to an initial state of membrane stresses, defined by N_x, N_y and N_{xy}.

3.5 Element Load Vector

The external loads considered for the bending problem may be independent or combination of the load cases that follow :

(a) concentrated nodal loads (P_c), acting in the direction of the corresponding nodal degree of freedom.

(b) uniformly distributed load (P_o) over the top or bottom faces of the element acting in z-direction.

The total external work done by these forces on an element can be expressed as :

$$W_p^e = d^T [\bar{P}_c + \int_A N^T \bar{P}_o \, dA] \qquad (3.26)$$

or

$$W_p^e = d^T P^e \qquad (3.27)$$

P^e is the element load vector and $\bar{P}_c = (\bar{P}_{c_1}^T, \bar{P}_{c_2}^T, \ldots \bar{P}_{c_{NN}}^T)^T$

where $\bar{P}_{c_i}$ is the vector of concentrated forces/couples at node i in the direction of nodal degrees of freedom.

$\bar{P}_0$ vector is defined as,

$$\bar{P}_0 = (\bar{P}_{0_1}{}^T, \bar{P}_{0_2}{}^T, \ldots \quad \bar{P}_{0_{NN}}{}^T)$$

where, $\bar{P}_{0_i}$ is given by,

for symmetric laminates :

$$\bar{P}_{0_i} = (P_0, 0, 0, 0, 0)^T$$

for unsymmetric laminates :

$$\bar{P}_{0_i} = (0, 0, P_0, 0, 0, 0, 0, 0, 0)^T \qquad (3.28)$$

3.6 Derivation of the Equilibrium Equations

The total potential of an element can be written as :

$$\pi^e = U^e - W^e \qquad (3.29)$$

Using Equation (3.1), the total potential of the whole structure can be written in general as follows :

$$\pi = \sum_{e=1}^{NEL} U^e - W^e \qquad (3.30)$$

U^e is the strain energy of the element given by the relation (3.14). W^e is the total work done by the external forces.

For the bending problem, the total external work done by applied forces is denoted as W_p^e given by the relation (3.27). Using the expressions (3.14) and (3.27) for strain energy and external work done respectively, the total potential for the bending case is,

$$\pi = \sum_{e=1}^{NEL} [(\tfrac{1}{2} d^T [K]^e d - d^T p^e] \tag{3.31}$$

minimization with respect to d leads to the following equilibrium equation system,

$$\sum_{e=1}^{NEL} [K]^e d = \sum_{e=1}^{NEL} p^e \tag{3.32}$$

which can be solved for the displacement vector 'd'.

For the buckling problem, the total external work done by a set of inplane loads is denoted as W_g^e, given by the relation (3.24). Using the expressions (3.14) and (3.24) for the strain energy and work done, the total potential for the buckling case is,

$$\pi = \sum_{e=1}^{NEL} [(\tfrac{1}{2} d^T [K]^e d) - (\tfrac{1}{2} d^T [G]^e d)] \tag{3.33}$$

For convenience, N_x, N_y and N_{xy} may be expressed in terms of a common load 'N', such that

$$N_x = \alpha \, N$$
$$N_y = \beta \, N$$
$$N_{xy} = \gamma \, N \tag{3.34}$$

Substituting in (3.25) and assuming the initial state of stresses to be uniform throughout the plane of the element, the geometric stiffness matrix can be written as

$$[G]^e = N \int_A \left[B_g^T \begin{bmatrix} \alpha & \gamma \\ \gamma & \beta \end{bmatrix} B_g \right] dA \tag{3.35}$$

$$= N \, [G']^e$$

The applied stresses are assumed to increase in proportion to a load factor 'f' upto the level when buckling occurs.[33] Therefore, at the point of buckling,

$$[G]^e = fN \, [G']^e \tag{3.36}$$

writing, $N_{cr} = fN,$ $\tag{3.37}$

$$[G]^e = N_{cr} \, [G']^e \tag{3.38}$$

At the point of instability, the total potential has a stationary value. Hence, using (3.38) in (3.33) and minimising π with respect to d, we get,

$$[[K]^e - N_{cr} [G']^e] \ d = 0 \tag{3.39}$$

which is a typical eigenvalue problem. On solving, the lowest magnitude eigenvalue gives the critical buckling load. The eigenvectors represent the buckled shape.

3.7 Evaluation of the Stiffness Matrices and Load Vectors

The integrals involved in the expressions for $[K]^e$, $[G']^e$ and P^e are evaluated using the Gauss-Quadrature. To achieve economy in computation, the element elastic stiffness matrix and the geometric stiffness matrix are partitioned in both the row and column directions into blocks. Each block corresponds to the degrees of freedom at a node. The expression for the stiffness matrix for a typical block ij can be written as,

$$K_{ij}^e = \int_{-1}^{1} \int_{-1}^{1} B_i^T \ D \ B_j \ |J| \ d\xi \ d\eta$$

or

$$K_{ij}^e = \sum_{f=1}^{m} \sum_{g=1}^{n} W_f \ W_g \ |J| \ B_i^T \ D \ B_j \tag{3.40}$$

Similarly,

$$G'^e_{ij} = \int_{-1}^{1} \int_{-1}^{1} B_{g_i}^T \begin{bmatrix} \alpha & \gamma \\ \gamma & \beta \end{bmatrix} B_{g_j} \ |J| \ d\xi \ d\eta$$

$$\text{or,} \ G'^e_{ij} = \sum_{f=1}^{NG} \sum_{g=1}^{NG} W_f \ W_g \ |J| \ B_{g_i}^T \begin{bmatrix} \alpha & \gamma \\ \gamma & \beta \end{bmatrix} B_{g_j} \tag{3.41}$$

in which W_f and W_g are the weighting coefficients, 'NG' is the number of numerical quadrature points in each of the directions ξ and η. $|J|$ represents the determinant of the standard Jacobian matrix that relates the shape function derivatives in the natural coordinates ξ and η with those of x and y coordinates. The subscripts i and j refer to the nodes that are related to block ij.

The matrices B_i and B_j are given in general as,

$$B_i = \begin{Bmatrix} B_{m_i} \\ B_{b_i} \\ B_{s_i} \end{Bmatrix} \quad \text{and} \quad B_j = \begin{Bmatrix} B_{m_j} \\ B_{b_j} \\ B_{s_j} \end{Bmatrix} \tag{3.42}$$

where the membrane terms are non-existent for symmetric laminates.

The computation of K_{ij} and G'_{ij} is economised by explicit multiplication of the triple products.[23] Also, due to symmetry of the stiffness matrix, the block K_{ij} lying on one side of the main diagonal are only formed. Each block in G'_{ij} contains only one one-zero term which only is required to be formed.

The evaluation of the load vector P^e defined in Equation (3.27) is also done using numerical integration by expressing as follows :

$$P^e = \bar{P}_c + \int_{-1}^{1} \int_{-1}^{1} N^T \bar{P}_o \, |J| \, d\xi \, d\eta$$

using Gauss quadrature,

$$P^e = \bar{P}_c + \sum_{f=1}^{NG} \sum_{g=1}^{NG} W_f W_g \, |J| \, N^T \bar{P}_o \qquad (3.43)$$

The exact integration of the integrals in the stiff-ness matrices requires 3x3 Gauss point integration rule. But, at the thin plate limit, this may lead to overstiff results. This is because, the shear energy terms in the elastic stiffness matrix $[K]^e$ acts as penalty function which constrain the shear-strains γ_{xz} and γ_{yz} to zero as plate thickness to span ratio is reduced. Therefore, a reduced 2x2 integration rule is normally used for evalua-ting shear energy terms to alleviate the overconstraining effect, while the full (3x3) integration is adopted for nonshear terms.

CHAPTER 4

RESULTS AND DISCUSSIONS

4.1 Preliminary Remarks

In this chapter, results for stress and stability
analysis using the present higher order theory for various
numerical examples drawn from available literature are
presented and discussed. The reliability of the present
finite element formulation, programme and applicability and
necessity of the higher order theory are examined by comparing
with the exact 3-dimensional elasticity solutions, closed
form solutions from higher order theories (denoted as HSDT),
first order shear deformation theory (denoted as FSDT) and
classical plate theory (denoted as CPT) results. In the
various examples, the parameters whose effect is examined
include boundary conditions, orthotropicity ratio, number of
layers, side to thickness ratio and fibre orientation.

The stresses are evaluated at the Gauss points nearest
to the concerned nodes. Unless stated otherwise the trans-
verse shear stresses and the geometric stiffness matrix are
evaluated at the reduced Gauss points. Unless otherwise
specified 3x3 mesh in quarter plate is used for bending and
2x2 mesh in quarter plate for buckling. The transverse shear
stresses are computed using equilibrium equations as well as

constitutive relations and presented. In a few cases, the effect of different integration schemes is also investigated. The computations are done on DEC-1090 system. A note on the computational work is presented in Appendix.

Unless otherwise stated, the deflections and stresses are non-dimensionalized as follows :

$$\bar{w} = \frac{wE_2h^3}{P_o a^4}$$

$$(\bar{\sigma}_x, \bar{\sigma}_y, \bar{\sigma}_{xy}) = \frac{(\sigma_x, \sigma_y, \sigma_{xy})\, h^2}{P_o a^2}$$

$$(\bar{\sigma}_{xz}, \bar{\sigma}_{yz}) = \frac{(\sigma_{xz}, \sigma_{yz})\, h}{P_o a}$$

$$(\bar{M}_x, \bar{M}_y, \bar{M}_{xy}) = (M_x, M_y, M_{xy})\, \frac{1}{P_o a^2}$$

$$(\bar{N}_x, \bar{N}_y, \bar{N}_{xy}) = (N_x, N_y, N_{xy})\, \frac{1}{P_o a}$$

$$\bar{N}_{cr} = \frac{N_{cr}\, b^2}{E_2 h^3} \tag{4.1}$$

The locations for the various quantities presented are as follows :

W_o, M_x, M_y : Centre of the plate at $z = 0.5$ h

σ_x, σ_y : Centre of the plate at $z = 0.5$ h

M_{xy}, σ_{xy} : Corner of the plate at $z = 0.5$ h

σ_{xz} : Mid edge along y-axis at $z = 0$

σ_{yz} : Mid edge along x-axis at $z = 0$

The positive set of stresses and stress resultants is shown in Figure 4.1.

4.2 Presentation of the Results and Discussions

The results are classified under two headings, as follows :

4.2.1 Stress analysis

    (a) Convergence study,

    (b) Orthotropic plates,   105829

    (c) Symmetric laminates,

    (d) Unsymmetric laminates,

    (e) Sandwich plates,

4.2.2 Stability analysis

    (a) Isotropic plates,

    (b) Orthotropic plates,

    (c) Symmetric laminates,

    (d) Unsymmetric laminates.

4.2.1 Stress analysis

4.2.1.a Convergence study

A simply supported 3-layer orthotropic laminates with different properties for the middle and outer layers is considered with the following data :

Properties for the middle layer : (in terms of stiffness coefficients)

(refer Eqn. 2.3)

$$\frac{\bar{C}_{22}}{\bar{C}_{11}} = 0.543103 \, , \qquad \frac{\bar{C}_{12}}{\bar{C}_{11}} = 0.23319, \qquad \frac{\bar{C}_{13}}{\bar{C}_{11}} = 0.010776$$

$$\frac{\bar{C}_{23}}{\bar{C}_{11}} = 0.098276 \, , \qquad \frac{\bar{C}_{33}}{\bar{C}_{11}} = 0.530172, \qquad \frac{\bar{C}_{44}}{\bar{C}_{11}} = 0.262931$$

$$\frac{\bar{C}_{55}}{\bar{C}_{11}} = 0.26681 \, , \qquad \frac{\bar{C}_{66}}{\bar{C}_{11}} = 0.159914$$

$$\vartheta_{12} = 0.44 \qquad h_m = 0.8 \, h$$

The properties of outer layer are defined by

$$R = \frac{\bar{C}_{outer}}{\bar{C}_{mid}} = 10, \quad a = b = 10 \text{ in.} \quad a/h = 10,$$

$$P_o = 100 \text{ psi}, \quad \bar{C}_{11} = 1.0 \qquad\qquad (4.2)$$

The convergence of the non-dimensionalized maximum deflection to the exact 3-D result [44] with mesh refinement is shown in Figure 4.2. The convergence of maximum $\bar{\sigma}_x$, $\bar{\sigma}_y$, $\bar{\sigma}_{xz}$ and $\bar{\sigma}_{yz}$ are also shown in the same figure. It can be

seen that for a 3x3 mesh in quarter plate, the results are convincingly accurate and further refinement does not seem to be necessary.

4.2.1.b Orthotropic plates

A simply supported square orthotropic plate with the following properties and subjected to uniform transverse pressure is considered for study.

E_1 = 20.83 x 10^6 psi, E_2 = 10.94 x 10^6 psi,

G_{12}= 6.10 x 10^6 psi, G_{23}= 6.19 x 10^6 psi,

G_{13}= 3.71 x 10^6 psi, ϑ_{12}= 0.44,

a = b = 10 in. , P_o = 100 psi   (4.3)

The results are presented in Table 4.1 for a/h ratios 10 and 20. The comparison is done with Reddy's higher order theory results [15] and exact 3-D elasticity results [44]. The results compare reasonably well. The shear stress values computed using equilibrium equations show some difference from the values computed using constitutive relations.

4.2.1.c Symmetric laminates

A 3-layered cross ply (0/90/0) laminate under uniformly distributed transverse loading is chosen for study. Thickness and material of all laminae are same showing the

orthotropic characteristics as follows :

$E_1 = 19.2 \times 10^6$ psi, $\quad E_2 = 1.56 \times 10^6$ psi,

$G_{12} = G_{13} = 0.82 \times 10^6$ psi, $\quad G_{23} = 0.523 \times 10^6$ psi,

$\vartheta_{12} = 0.24$, $\quad$ a = b = 10 in. $\hspace{4cm}$ (4.4)

The edges y = 0, b are considered invariably simply
supported while x = 0, a are considered SS, CC, FF, SC and
FS (S, F and C denoting a simply supported, a free and a
clamped edge respectively).

For comparison sake, the results for SS, CC and FF
boundary condition cases are shown in Tables 4.2 to 4.4.
The results from another HSDT [22], FSDT [22] and CPT [22]
are presented along with for comparison. The present
results closely compare with the HSDT results. The stress
values obtained from the higher order theories and FSDT
exhibit appreciable difference which are more significant
when a/h ratio decreases. But, $\bar{w}$ values computed by the two
approaches show little difference between them. The classi-
cal plate theory (CPT) results compare only for b/h = 20,
when shear deformation becomes negligible.

Figure 4.3 reveals that the transverse shear effects
are appreciable for moderately thick to thick plates,
irrespective of the type of boundary conditions. In
Figures 4.4 and 4.5 the non-dimensional normal stresses are

plotted vs side to thickness ratio and compared with FSDT and CPT results. It is observed that for increasing side to thickness ratio, the FSDT solution converges from below, while the higher order theory solution converges from above.

The variation of stresses through the laminate thickness is displayed in Figures 4.6 to 4.8 for a/h = 10 for varying boundary conditions. It can be seen that the transverse shear stresses predicted by the present theory are non-vanishing at the bounding surfaces. All the same, their values are relatively insignificant. As is seen from Fig. 4.8, the shear stresses computed using constitutive relations violate the interface continuity. The shear stresses computed using equilibrium equations provide a continuous variation.

4.2.1.d Unsymmetric laminates

The flexural behaviour of a 2-layered simply supported angle ply laminate under uniform transverse pressure is studied. The properties and thickness for each layer remain the same. The following data is used :

$$E_1 = 40 \times 10^6 \text{ psi}, \quad E_2 = 10^6 \text{ psi}, \quad G_{12} = 0.5 \times 10^6 \text{ psi},$$

$$G_{23} = G_{31} = 0.6 \times 10^6 \text{ psi}, \quad \vartheta_{12} = 0.25, \quad a = b = 10 \text{ in.}$$

$$P_o = 100 \text{ psi.}$$

The nondimensionalized maximum deflection and stress resultants obtained from the present theory are compared with results from Ren's closed form solutions of HSDT [18] for a/h = 10, 100 and classical plate theory [18] for a/h = 100, for different fibre orientations. As seen from Table 4.5, the present results compare well with the closed form solutions of the Ren's higher order theory. For thin plates, they converge to the classical plate theory results.

It is seen from the results that the deflection values do not vary appreciably with the fibre orientations. But, the values of $\bar{N}_x$, $\bar{N}_y$, and $\bar{N}_{xy}$ drastically reduce to a low value for $\alpha = 45^o$. This indicates that the coupling effect is considerably less for $\alpha = 45^o$.

4.2.1.e Sandwich plates

Example 1 : A simply supported square sandwich plate with aluminium faces and balsa core subjected to uniform transverse pressure is studied with the following face properties:

$$E_f = 10 \times 10^6 \text{ psi}, \quad t_f = 0.032 \text{ in.} \qquad (4.5)$$

The objective of the study is to establish the applicability of the present theory to the analysis of sandwich plates, by comparing with available test [45] results. The results are presented in Tables 4.6 and 4.7 for varying spans, core thickness, core shear rigidity and load intensities. The present results compare satisfactorily with

the test results. Since all the plates considered therein fall within the thin plate domain, only slight improvement is found in some of the cases over the first order theory results [45] (also presented). It is further observed that when the core shear rigidity is low, the consideration of face shear rigidity yields better deflection values in majority of the cases. Though this does not lead to a clear conclusion in this regard, because of the number of parameters varied, it prompts us for a more systematic investigation, which is done in the next example.

Example 2 : A simply supported square sandwich plate with the following properties is taken for study :

Face : $E_1/E_2 = 25$, $E_2 = 10^6$ psi, $\dfrac{G_{12}}{E_2} = \dfrac{G_{13}}{E_2} = 0.5$,

$\dfrac{G_{23}}{E_2} = 0.2$, $\nu_{12} = 0.25$.

Isotropic core : $E = 0$, G_c is defined by $R = \dfrac{G_{23_f}}{G_c}$

$a = b = 10$ in., $P_o = 100$ psi, $a/h = 10$ (4.6)

mesh : 2 x 2 in quarter plate.

The effect of considering the shear rigidity of faces, on the computed response is studied for varying core to face thickness ratio (C/t) and 'R' values. The results are

displayed in Table 4.8. It can be noticed that as c/t ratio increases, for any 'R' value, the effect of considering shear rigidity of faces diminishes. This is because, as the face becomes relatively thinner, the transverse shear effects in the face become less and less significant. Secondly, it is predominantly seen that as R increases, i.e., as the transverse shear rigidity of core relative to the shear rigidity of face decreases, the consideration of face shear rigidity makes a marked change in the results. This is more so for thicker faces. The explanation can be that when the core is relatively weak in shear, the resistance of the faces to transverse shear deformation become relatively more signi-ficant and effective. The effect of considering the shear rigidity of faces is not predominant when core shear rigidity is high, as due to the fact that the faces are relatively thin and their shear resistance will become insignificant compared to that of the thick, rigid core.

Example 3 : A simply supported sandwich panel with thin faces is taken for study with the properties mentioned below.

face : $E_f = 10 \times 10^6$ psi, $\nu_f = 0.3$, $t_f = 0.005$ in.

core : $G_c = 10,000$ psi, $t_c = 0.4$ in.

$$\nu_b = 1.0 \text{ in.} \tag{4.7}$$

The maximum deflection and stresses are computed using the present theory and shown in Table 4.9 along with results from Allen [46]. The results compare well for both aspect ratios. The effect of integration scheme on the computed values is also studied. It is found from the Table 4.8 that for the relatively thick plate that is considered in the problem, the order of integration does not have a pronounced effect on the values, for the element under consideration.

Example 4 : Rectangular sandwich plates with laminated faces of size 18 in. ×12 in.   are considered for study. The data used follows :

CFRP face plate : 3 layers each of thickness 0.005 in. for
each face plate.

$$E_1 = 15.2 \times 10^6 \, psi, \quad E_2 = 1.26 \times 10^6 \, psi;$$
$$G_{12} = 0.66 \times 10^6 \, psi, \quad \nu_{12} = 0.327$$

aluminium honey-comb core :

$$G_{13} = 14.91 \times 10^3 \, psi, \quad G_{23} = 9.0 \times 10^3 \, psi,$$
$$P_o = 0.1462 \, psi.$$

Four types of lay ups are considered for the specimens for which experimental results are available.

SP1 : $[30_3/core/30_3]$, SP2 : $[0_3/core/0_3]$

SP3 : $[30/-30/30/core/30/-30/30]$

SP4 : $[0/90/0/core/0/90/0]$

The core thickness for SP1 and SP2 is 10 mm, while for SP3 and SP4, it is 7 mm. (4.8)

The results are displayed along with the experimental [47] and FSDT results [47] in Table 4.10. The deflections are computed for both simply supported (SS) and clamped (CC) boundary conditions, as the test boundary conditions are stated to be in between the two types, but intended to be clamped. It is seen that the higher order theory results for the clamped condition are closer to the experimental results than the FSDT results. But, there is considerable difference between the experimental results and the present results. The reason is that the clamped boundary conditions were not satisfactorily achieved during experimentation, as stated in the reference.[47].

4.2.2 Stability analysis

4.2.2.a Isotropic plates

A simply supported, square isotropic plate is considered with properties and other data as given below :

$$E = 2.5 \times 10^6 \text{ psi}, \quad \nu = 0.25, \quad a = b = 10 \text{ in.} \quad (4.9)$$

The uniaxial buckling loads are computed. The results are displayed in nondimensionalized form in Figure 4.9 along with exact 3-D elasticity [35] and classical plate theory [35] results. The figure exhibits the close agreement of

of the results computed using the higher order theory with the 3-D elasticity results for range of plates from thick to thin. The mesh used for computing the values being 2 x 2 in quarter plate, it can be expected that as mesh is refined, the agreement with the exact solutions will be more remarkable. It is clearly seen that as the plate thickness increases the buckling parameter decreases. This is because of the transverse shear deformation that becomes predominant for thicker plates. The classical plate theory which neglects the transverse shear effects is found to be erroneous for thicker plates.

4.2.2.b Orthotropic plates

A simply supported square plate with the following orthotropic properties in the form of ratios of stiffness coefficients is treated for study :

$$\frac{C_{22}}{C_{11}} = 0.543103, \quad \frac{C_{12}}{C_{11}} = 0.23319, \quad \frac{C_{13}}{C_{11}} = 0.010776$$

$$\frac{C_{23}}{C_{11}} = 0.098276, \quad \frac{C_{33}}{C_{11}} = 0.530172, \quad \frac{C_{44}}{C_{11}} = 0.262931,$$

$$\frac{C_{55}}{C_{11}} = 0.26681,$$

$$a = b = 10 \text{ in.}, \quad C_{11} = 1.0 \tag{4.10}$$

The nondimensionalized uniaxial critical buckling load
is plotted versus a/h ratio in Figure 4.9. The exact elasti-
city [44], Mindlin's [44] and CPT [44] results are also shown
for comparison. Once again, $\overline{N}_{cr}$ decreases with increase in
a/h ratio which can be attributed to the influence of the
transverse shear deformation. The thin plate theory is seen
to provide optimistic values of buckling load, the errors
increasing with thickness. The thin plate assumptions
increase the stiffness of the structure, thus yielding higher
values.

4.2.2.c Symmetric laminates

A simply supported symmetric cross ply laminate is
studied. The following data is used :

$$\frac{G_{13}}{E_2} = \frac{G_{12}}{E_2} = 0.6, \quad \frac{G_{23}}{E_2} = 0.5, \quad \nu_{12} = 0.25, \quad E_2 = 10^6 \text{ psi.}$$

$$a = b = 10 \text{ in.,} \quad a/h = 10 \tag{4.11}$$

The nondimensionalized critical buckling parameter is
evaluated for different number of layers and different
degrees of orthotropy. The values are shown in Table 4.11.
The comparison is done with a HSDT [39], FSDT [39] and
CPT [39] results. The present results match closely with
the HSDT result. For the moderately thick plate that is
studied, the response is not significantly different from the
FSDT results. Probably, the effects of the assumptions of

higher order theory can be felt for thicker plates. It is observed that the CPT results overestimate the buckling load. The error increases with increase in orthotropicity ratio.

It can be noticed that the integration rule adopted has very slight effect on the results. Still, the results obtained from full integration are consistently slightly higher than their counterparts. This is due to the over-stiffening effect when the shear terms of the stiffness matrix are formed using full integration.

Figure 4.10 displays the variation of buckling parameter with degree of orthotropy. The buckling parameter is found to increase with the degree of orthotropy. Further, from Table 4.11, it is seen that the number of layers does not appreciably affect the critical buckling load. However, for higher orthotropicity ratio, there is a slight noticeable increase in the values with increase in number of layers.

4.2.2.3 Unsymmetric laminates

Example 1 : A simply supported square antisymmetric cross ply laminate is considered for study, with the properties of individual laminae and other data as in 4.11.

The Table 4.12 is devoted to the comparison of the uni-axial buckling parameter $(\overline{N}_{cr})$ obtained from the present approach with those available in literature, and to emphasise the effect of inplane orthotropicity ratio and number of

layers. The present results compare better than the Reddy's HSDT results [37], with the exact 3-D elasticity results by Noor [48], especially for higher degrees of orthotropy. The numerical results allow one to infer that for a thick plate, and when material exhibits high ortho-tropicity ratio, the effect of transverse shear deformation needs to be incorporated. It can also be remarked that the difference between the classical buckling load on one hand and their shear deformation theory counterparts on the other, increases drastically for high orthotropicity ratio, as the number of layers increase. The $\bar{N}_{cr}$ values, in general, increase remarkably with increase in number of layers from 2 to 4, but thereafter, marked increase is not noticed. This behaviour is due to the fact that, when there are two layers, the coupling between extension and bending is maximum, leading to a decrease in the buckling load. With increase in number of layers to four, the coupling effect is significantly reduced, thereby increasing the buckling load. With further increase in number of layers this reduction is relatively less drastic. A comparison between Tables 4.11 and 4.12 also reveals the role of coupling in bringing down the buckling strength, the effect becoming less significant for larger number of layers.

Example 2 : A simply supported, square, antisymmetric angle
ply laminate with the following properties is studied for
response to uniaxial uniform compresive loading.

$$E_2 = 10^6 \text{ psi}, \quad G_{12}/E_2 = 0.6, \; G_{23}/E_2 = G_{31}/E_2 = 0.5,$$

$$\nu_{12} = 0.25, \quad a = b = 10 \text{ in.} \;, \text{ Numbers of layers} = 2 \quad (4.12)$$

The uniaxial buckling parameter $\bar{N}_{cr}$ for varying fibre
orientation and degree of orthotropy are computed and shown
in Tables 4.13 and 4.14 for a/h = 10 and 100 respectively.
The results match well with the results from available
HSDT [41] for all fibre orientations and orthotropicity
ratios. The $\bar{N}_{cr}$ values increase with increase in inplane
orthotropicity ratio for all fibre orientations, and side to
thickness ratios. For $\Theta = 5^\circ$, this trend is most pronounced,
as the fibres being closer to the axis of loading, any
increase in the strength along the fibres will be more signi-
ficantly reflected along the loading axis. A comparative
study between the Tables 4.12 and 4.13 reveals that the
buckling parameter values decrease with increase in thickness
the shear deformation effects being the cause.

CHAPTER 5

CONCLUSIONS

5.1 General

A higher order shear deformation theory for the bending
and buckling analysis of laminated composite plates is
presented. Certain general conclusions can be drawn from its
application to numerous examples.

*   The displacement based finite element formulation for the
buckling analysis of laminated composite plates using a higher
order displacement model had not been attempted so far in the
literature. The various numerical examples worked out indicate
the reliability of the present formulation. The close agreement
of the results with exact solutions makes it acceptable for
general use in the analysis of the stability of laminated
composite plates.

*   The formulation for the stress analysis has been tested
for various boundary conditions in Section 4.2.1.c. Also,
in Section 4.2.1.d, examples worked out for unsymmetric
laminates for varying fibre orientations and side to thickness
ratios have close agreement with closed form solutions of higher
order theory. The consistently accurate results lead to the
conclusion that the present theory is applicable to a wide
range of problems associated with bending of laminated composite
plates.

*   The adaptability of the present formulation to sandwich
plate problems is thoroughly investigated in Section 4.2.1.e.
The parameters involved include varying core and face properties
and various combinations of fibre orientations for the CFRP
faces.   The satisfactory results obtained allow us to be confi-
dent about the predictive capability of the higher order theory
with regards to stress analysis of sandwich plates.

*   In Section 4.2.1.e, example 2 was devoted to a systematic
examination of the effect of considering the shear rigidity of
faces in sandwich plate analysis.   The study reveals the
follows :

(a) For sandwich plates with thin faces ($c/t > 50$), considera-
tion of the shear rigidity of faces has no significant effect,
even with relatively weak cores.

(b) For thicker faces, when the shear rigidity of faces is high
relative to that of the core ($R > 10$ approximately), the neglect
of face transverse shear leads to high, erroneous deflection
values.

(c) The moment resultant values are generally not much affected
by the face shear considerations.

      In general, it can be concluded that the face shear rigidity
is to be accounted in the deflection analysis of sandwich plates,
except for the case of very thin face and cores with high shear
rigidity.

* As can be seen from the results in Tables 4.2 to 4.4 , the first order shear deformation theory is satisfactory for the deflection calculations. But, for thick laminates, the stress values from FSDT are highly erroneous and it becomes inevitable to resort to the higher order shear deformation theory. The classical laminate theory can be relied upon in the thin plate (a/h > 20) domain only. Even there, it lacks the capacity to predict the transverse shear stresses.

The FSDT results for the uniaxial critical buckling load for symmetric cross ply laminated plates is given in Table 4.11. For the type of laminate studied, it can be seen that the first order shear deformation theory will suffice to determine the lowest buckling load. Again, the classical plate theory is not reliable for thick plates, the error increasing with degree of orthotropy.

* It is clear from Tables 4.9 and 4.11 that the type of integration adopted has little effect on the results when the 9-noded Lagrangian element is used either for the stress analysis of sandwich plates or buckling response of a laminate.

5.2 Recommendations for Future Work

Some of the future work that can be carried out as an extension or improvement over the present investigation are suggested below.

With some effort, this work can be extended to the stress analysis of stiffened laminated plates and laminated composite shells. The response to combined transverse and inplane loading has not been studied in the present investigation. This can be included in a future work. The present work can form the basis for a formulation for the nonlinear analysis.

The buckling formulation and program that is developed can be utilized to analyze the stability of sandwich plates. The program also caters for biaxial and shear buckling of laminated composite plates. These could be investigated in a future work. Formulation can be developed for buckling due to combined transverse and inplane loads including shear.

An improvement over the buckling formulation presented is to consider all the components of the nonlinear strains such as,

$$\Theta_x = \frac{\partial u}{\partial x} + \frac{1}{2} \left[(\frac{\partial u}{\partial x})^2 + (\frac{\partial v}{\partial x})^2 + (\frac{\partial w}{\partial x})^2 \right], \text{ etc.,}$$

in forming the initial stress matrix. The problem becomes more involved. A stress analysis may have to be carried out to determine the stress distribution and the results used to form the initial stress matrix.

ee: Equillibrium Equation   cr: Constitutive Relation

HSDT: Reddy's Theory   Exact: 3-D Elasticity Results

a/h	Source	$\bar{W}$	$\bar{\sigma}_y$	$\bar{\sigma}_{xz}^{cr}$	$\bar{\sigma}_{xz}^{ee}$
10	Present	0.03081	0.3618	0.5003	0.44467
	HSDT	0.03080	0.3608	0.5423	—
	Exact	0.03078	0.3608	0.5427	—
20	Present	0.03253	0.3615	0.5013	0.4438
	HSDT	0.03251	0.3601	0.5332	—
	Exact	0.03247	0.3602	0.5341	—

Table 4.1 : Maximum deflection and stresses in an orthotropic panel

HSDT : Khdeir's Theory   Cr: Constitutive Relation;   ee: Equillibrium Equation

a/h	Source	$\bar{w}$	$\bar{\sigma}_x$	$\bar{\sigma}_y$	$\bar{\sigma}_{yz}$ cr	$\bar{\sigma}_{yz}$ ee
2	Present	0.07131	0.6997	0.5492	0.4075	0.5726
	HSDT	0.07258	0.4651	0.5628	0.4715	---
	FSDT	0.07058	0.5020	0.5984	0.3245	---
	CPT	0.01206	0.7251	0.1933	0.0000	---
5	Present	0.02355	0.7644	0.3422	0.3216	0.2914
	HSDT	0.02324	0.7435	0.3370	0.3578	---
	FSDT	0.02273	0.6551	0.3302	0.2528	---
	CPT	0.01206	0.7251	0.1933	0.0000	---
10	Present	0.01510	0.7365	0.2390	0.2870	0.2511
	HSDT	0.01499	0.7284	0.2371	0.3191	---
	FSDT	0.01484	0.7036	0.2342	0.2270	---
	CPT	0.01206	0.7251	0.1933	0.0000	---
20	Present	0.01284	0.7309	0.2051	0.2775	0.2390
	HSDT	0.01280	0.7256	0.2048	0.3083	---
	FSDT	0.01277	0.7196	0.2042	0.2199	---
	CPT	0.01206	0.7251	0.1933	0.0000	---

Table 4.2 : Maximum deflection and stresses in a 3-layered cross-ply laminate under uniform transverse pressure. (SS boundary conditions)

cr: Constitutive Relation
ee: Equillibrium Equation

H S D T : Khdeir's Theory

a/h	Source	$\bar{w}$	$\bar{\sigma}_x$	$\bar{\sigma}_y$	$\bar{\sigma}_{yz}{}^{cr}$	$\bar{\sigma}_{yz}{}^{ee}$
2	Present	0.06309	0.5877	0.4995	0.3670	0.3330
	HSDT	0.06966	0.7214	0.5617	0.4505	—
	FSDT	0.06706	0.1969	0.5873	0.3115	—
	CPT	0.00280	0.2787	0.0185	0.0000	—
5	Present	0.01598	0.3923	0.2209	0.2452	0.2112
	HSDT	0.01655	0.3717	0.2319	0.2848	—
	FSDT	0.01580	0.2593	0.2183	0.1988	—
	CPT	0.00280	0.2787	0.0185	0.0000	—
10	Present	0.00651	0.3193	0.0773	0.1853	0.1440
	HSDT	0.00653	0.3094	0.0790	0.2160	—
	FSDT	0.0063	0.2786	0.0741	0.1525	—
	CPT	0.0028	0.2787	0.0185	0.0000	—
20	Present	0.0038	0.2950	0.0317	0.1619	0.1179
	HSDT	0.0038	0.2882	0.0327	0.1910	—
	FSDT	0.0037	0.2802	0.0316	0.1359	—
	CPT	0.0029	0.2787	0.0185	0.0000	—

Table 4.3: Maximum deflection and stress in a 3-layered crossply
laminate under uniform transverse pressure.
(CC boundry conditions)

HSDT:Khdeir's Theory   ee: Equilibrium Equation

cr: Constitutive Relation

a/h	source	$\bar{w}$	$\bar{\sigma}_x$	$\bar{\sigma}_y$	σ_{yz}^{cr}	σ_{yz}^{ee}
2	Present	0.2037	0.0249	1.9648	0.8440	0.9040
	HSDT	0.2029	0.0277	1.9884	0.8860	—
	FSDT	0.2033	0.0033	2.1755	0.6330	—
	CPT	0.1092	0.0195	2.1597	0.0000	—
5	Present	0.1245	0.0183	2.1420	0.8700	0.9280
	HSDT	0.1242	0.0164	2.1349	0.8798	—
	FSDT	0.1243	0.0122	2.1646	0.6282	—
	CPT	0.1092	0.0195	2.1597	0.0000	—
10	Present	0.1130	0.0187	2.1660	0.8762	0.9786
	HSDT	0.1129	0.0173	2.1535	0.8780	—
	FSDT	0.1129	0.0161	2.1610	0.6264	—
	CPT	0.1092	0.0195	2.1597	0.0000	—
20	Present	0.1101	0.0193	2.1713	0.8773	0.9822
	HSDT	0.1101	0.0182	2.1581	0.8775	—
	FSDT	0.1101	0.0179	2.1600	0.6264	—
	CPT	0.1092	0.0195	2.1597	0.0000	—

table 4.4: Maximum deflection and stress in a 3-layered crossply laminate under uniform transverse pressure. (FF boundry conditions)

HSDT: Ren's Theory

a/h		Source	$\bar{W}$	$\bar{N}_x$	$\bar{N}_y$	$\bar{N}_{xy}$	$\bar{M}_x$	$\bar{M}_y$	$\bar{M}_{xy}$
10	15	Present	0.9294	0.4209	0.4298	0.3906	0.1121	0.01314	-0.01451
		HSDT	0.9845	0.4346	0.4414	0.4062	0.1133	0.01374	-0.01513
	30	Present	0.9592	0.2725	0.3083	0.3037	0.06918	0.02705	-0.03327
		HSDT	1.0354	0.2852	0.3329	0.3229	0.0700	0.02762	-0.03254
	45	Present	0.9094	0.0567	0.0567	0.0446	0.03654	0.03654	-0.04425
		HSDT	0.9894	0.0610	0.0610	0.0487	0.03663	0.03663	-0.04412
100	15	Present	0.7164	0.4360	0.4563	0.4190	0.1150	0.01235	-0.01503
		HSDT	0.7169	0.4409	0.4565	0.4136	0.1142	0.01234	-0.01522
		CPT	0.7142	0.4403	0.4567	0.4136	0.1142	0.01233	-0.01524
	30	Present	0.7773	0.2359	0.3064	0.3125	0.06980	0.02689	-0.03498
		HSDT	0.7779	0.2336	0.3066	0.3094	0.06954	0.02682	-0.03529
		CPT	0.7752	0.2321	0.3062	0.3092	0.06954	0.02681	-0.03539
	45	Present	0.7342	0.0464	0.0464	0.0449	0.03685	0.03685	-0.04601
		HSDT	0.7348	0.0465	0.0465	0.0446	0.03679	0.03679	-0.04630
		CPT	0.7321	0.0462	0.0462	0.0446	0.03680	0.03680	-0.04638

Table 4.5: Maximum deflection and stresses in a two layered simply supported angle-ply laminate under uniform transverse pressure.

A: Gf not considered; B: Gf considered; FSDT: NACA TN 2581 Theory

Side of plate (in inches)	C	Po (psi)	Wmax (inches)		
			Test value	FSDT	Present value
44.20	0.514	0.5408	0.168	0.171	A 0.172
					B 0.167
	0.390	0.7211	0.359	0.377	A 0.378
					B 0.366
32.04	0.507	0.7211	0.072	0.069	A 0.071
					B 0.065
	0.381	0.7211	0.112	0.111	A 0.112
					B 0.106
28.04	0.503	0.5768	0.035	0.034	A 0.034
					B 0.032
	0.388	0.7211	0.065	0.066	A 0.067
					B 0.062
21.97	0.512	1.803	0.046	0.042	A 0.043
					B 0.039
	0.390	1.082	0.044	0.040	A 0.041
					B 0.036

Table 4.6: Sandwich Plates: Comparison with test values. (Gc=12670 Psi)

A: Gf not considered; B: Gf considered; FSDT: NACATN 2581 Theory

Side of plate (in inches)	C	Po (psi)	Test value	FSDT	Present value	
44.20	0.755	0.721	0.110	0.114	A	0.126
					B	0.118
	0.637	0.721	0.158	0.155	A	0.170
					B	0.158
38.04	0.751	0.721	0.072	0.065	A	0.074
					B	0.068
	0.632	0.721	0.087	0.089	A	0.10
					B	0.091
28.04	0.752	0.721	0.024	0.021	A	0.026
					B	0.023
	0.633	0.721	0.030	0.029	A	0.035
					B	0.029
21.97	0.754	2.884	0.039	0.038	A	0.048
					B	0.040
	0.636	2.163	0.037	0.035	A	0.047
					B	0.038

Wmax (inches)

Table 4.7: Sandwich Plates: Comparison with test values. (Gc = 5840 psi)

A: G_f not considered ;   B: G_f considered

c/t			R = 2	4	10	20	40
10	$\bar{w}$	A	0.0317	0.0461	0.0855	0.1427	0.2454
		B	0.0271	0.0373	0.0635	0.0978	0.1486
	$\bar{M}_x$	A	0.1276	0.1211	0.1061	0.0911	0.0771
		B	0.1295	0.1260	0.1142	0.1033	0.0937
20	$\bar{w}$	A	0.0353	0.0534	0.0919	0.1485	0.2490
		B	0.03789	0.0486	0.0785	0.1228	0.1991
	$\bar{M}_x$	A	0.1309	0.1274	0.1177	0.1053	0.0902
		B	0.1314	0.1288	0.1211	0.1107	0.0973
50	$\bar{w}$	A	0.0719	0.0852	0.1235	0.1832	0.2922
		B	0.0706	0.0816	0.1133	0.1624	0.2539
	$\bar{M}_x$	A	0.1326	0.1314	0.1272	0.1202	0.1089
		B	0.1327	0.1317	0.1287	0.1226	0.1126
100	$\bar{w}$	A	0.1259	0.1389	0.1776	0.2397	0.3566
		B	0.1249	0.1307	0.1691	0.2211	0.3194
	$\bar{M}_x$	A	0.1330	0.1326	0.1307	0.1271	0.1120
		B	0.1330	0.1325	0.1311	0.1282	0.1222

Table 4.8 . Sandwich plates: Study of the effect of considering shear rigidity of faces.

78

Cr: Constitutive Relation   ee: Equillibrium Equation

a/b	source	type of integration	$\bar{w}_3$	$\bar{\sigma}_x$	$\bar{\sigma}_y$	$\bar{\sigma}_{xy}$	$\bar{\tau}_{xz}^{cr}$	$\bar{\tau}_{xz}^{ee}$	$\bar{\tau}_{yz}^{cr}$	$\bar{\tau}_{yz}^{ee}$
1	present	full	13.3247	3.9840	3.9840	2.6405	0.3457	0.2710	0.3557	0.2710
		mixed	13.3279	3.9840	3.9840	2.6214	0.3295	0.2680	0.3295	0.2685
		reduced	13.3280	3.9436	3.9346	2.5575	0.3295	0.2688	0.3295	0.2688
	allen		12.5357	4.0626	4.0626	2.5887	0.3465	---	0.3465	---
3	present	full	23.0166	3.3679	9.9142	3.8485	0.3030	0.2306	0.4707	0.4159
		mixed	23.0090	3.3686	9.9174	3.7591	0.2760	0.2172	0.4539	0.4155
		reduced	23.0088	3.3591	9.7999	3.6064	0.2761	0.2191	0.4469	0.4075
	allen		24.1038	4.0386	10.6193	3.1771	0.3516	---	0.4951	---

Table 4.9: sandwich plates: comparision for maximum deflection and stresses

CC: All edges clamped; SS: All edges simply supported.

specimen	test value (CC)	FSDT CC	SS	PRESENT CC	SS
SP1	69	50.4	117.3	52.8389	207.165
SP2	85	54.0	182.9	56.5056	178.603
SP3	94	77.2	179.4	80.5326	197.638
SP4	90	61.3	220.6	64.4510	216.010

TABLE 4.10: Sandwich plates with composites faces:
A comparision with test results

HSDT: Khdeir's Theory

No of Layers	Source	Type of integration	L/h				
			5	10		20	40
3	Present	Full	5.426	9.872	14.929	18.916	22.157
		Mixed	5.396	9.844	14.904	18.893	22.136
	HSDT		5.362	9.846	14.917	18.912	22.154
	FSDT		5.396	9.871	14.985	19.027	22.315
	CPT		5.754	11.492	19.712	27.936	36.160
5	Present	Full	5.444	10.123	15.796	20.547	24.598
		Mixed	5.413	10.094	15.771	20.526	24.579
	HSDT		5.406	10.078	15.747	20.503	24.568
	FSDT		5.407	10.076	15.736	20.485	24.547
	CPT		5.754	11.492	19.712	27.936	36.160
9	Present	Full	5.450	10.215	16.124	21.177	25.553
		Mixed	5.414	10.184	16.097	21.154	25.533
	HSDT		5.412	10.170	16.077	21.131	25.511
	FSDT		5.412	10.168	16.068	21.117	25.495
	CPT		5.754	11.492	19.712	27.936	36.160

Table 4.11: Nondimensionalised uniaxial critical buckling
load for symmetric cross-ply laminated plates.

HSDT: Reddy's Theory   Exact:Noor's 3-D elasticity

NO. of layers	Source	E1/E2				
		3	10	20	30	40
2	Present	4.7812	6.2671	8.0547	9.7130	11.2747
	Exact	4.6948	6.1181	7.8196	9.3746	10.8167
	HSDT	4.7749	6.2721	8.1151	9.8695	11.5630
	CPT	---	6.7030	8.8160	10.8910	12.9570
4	Present	5.2567	9.1943	14.0793	18.2936	21.9698
	Exact	5.1738	9.0164	13.7429	17.7829	21.2796
	HSDT	5.2523	9.2315	14.2540	18.6670	22.5790
6	Present	5.3475	9.7604	15.2603	17.9989	24.1252
	Exact	5.2673	9.6051	15.0014	19.6394	23.6689
	HSDT	5.3420	9.7762	15.3520	20.2010	24.4600
10	Present	5.3946	10.0571	15.8887	20.1890	25.3033
	Exact	5.3159	9.9134	15.6685	20.6347	24.9636
	HSDT	5.3882	10.0560	15.9140	20.9860	25.4220
	CPT	---	11.3000	19.2770	27.2540	35.2320

Table 4.12: Nondimensionalised uniaxial critical buckling load
   for antisymmetric cross-ply laminated plate.

HSDT : Ren's theory

	Source	3	10	20	30	40
				E_1/E_2		
0						
5	Present	5.3490	9.4797	13.8442	17.0683	19.5633
	HSDT	5.3890	9.7020	14.4174	18.0059	20.8422
15	Present	5.2731	8.6459	11.8467	14.1950	16.0825
	HSDT	5.3081	8.7884	12.1370	14.6057	16.5880
30	Present	5.1603	8.0615	11.0458	13.5990	15.7400
	HSDT	5.1872	8.1269	11.1235	13.6057	15.7517
45	Present	5.1321	8.1625	11.3768	14.1242	16.5468
	HSDT	5.1561	8.2138	11.4151	14.1103	16.4558

Table 4.13 : Nondimensionalised uniaxial critical buckling load for antisymmetric angleply square laminated plate. (a/h=10)

HSDT: Ren's Theory

θ	Source	E1/E2				
		3	10	20	30	40
5	Present	5.7422	11.2167	18.6018	25.5281	32.0543
	HSDT	5.7350	11.2040	18.5844	25.5119	32.0411
15	Present	5.6462	9.9050	14.6155	18.5615	22.0908
	HSDT	5.6386	9.8921	14.5982	18.5419	22.0682
30	Présent	5.5013	8.9796	12.9942	16.7940	20.5075
	HSDT	5.4942	8.9669	12.9770	16.7706	20.4793
45	Present	5.4628	9.0689	13.3714	17.5402	21.6685
	HSDT	5.4566	9.0570	13.3545	17.5169	21.6384

Table 4.14: Nondimensionalised uniaxial buckling load for antisymmetric (a/h = 100) angleply square laminated plate.
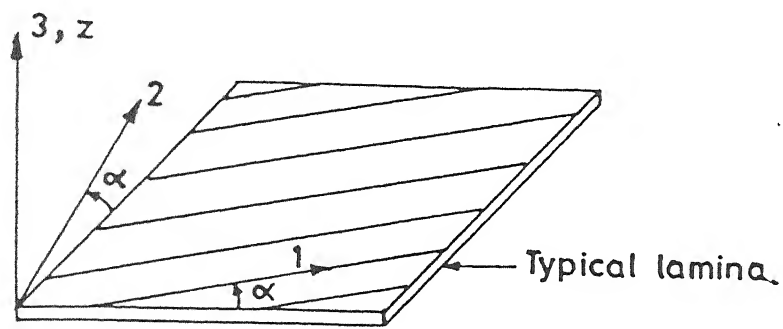
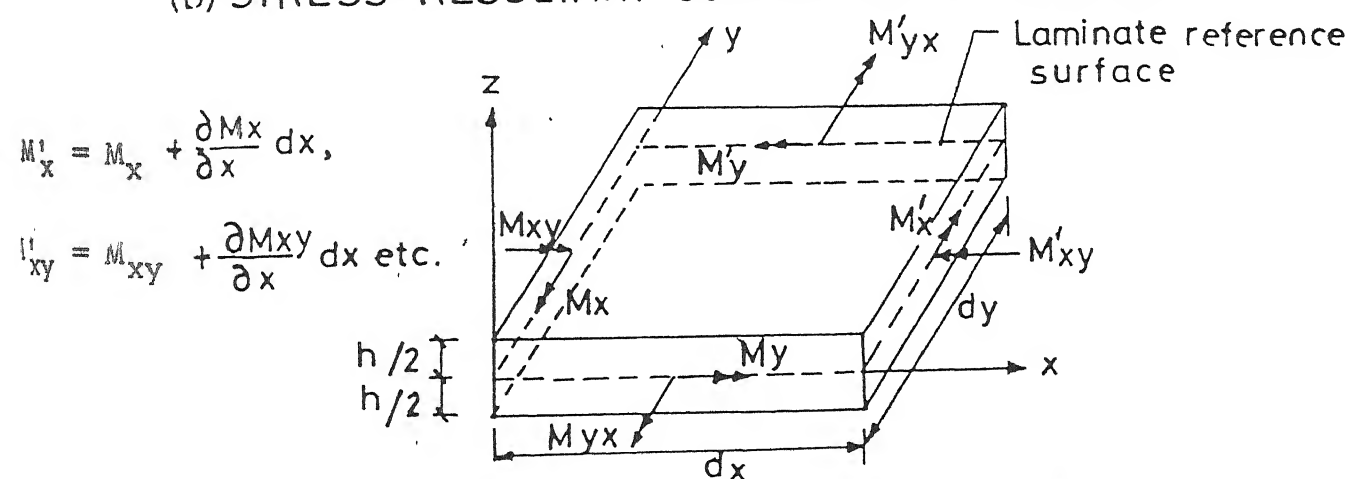(1, 2, 3) - Lamina reference axes
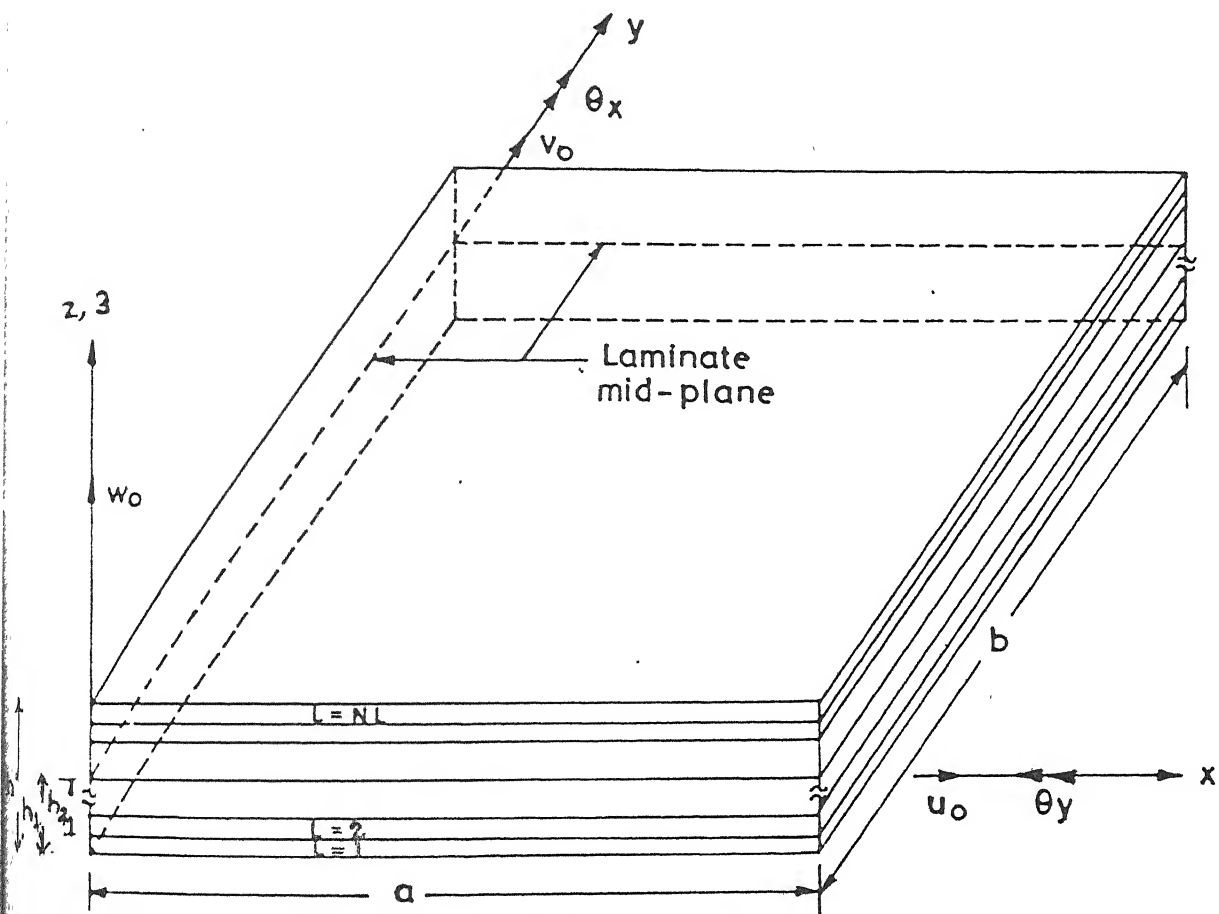
(x, y, z) - Laminate reference axes

Fig. 2.1 LAMINATE GEOMETRY WITH POSITIVE SET OF
LAMINA / LAMINATE REFERENCE AXES, DISPLACEMENT
COMPONENTS AND FIBRE ORIENTATION.

$\sigma'_x = \sigma_x + \dfrac{\partial \sigma x}{\partial x} dx,$

$\sigma'_{yz} = \sigma_{yz} + \dfrac{\partial \, yz}{\partial y} dy, etc.$
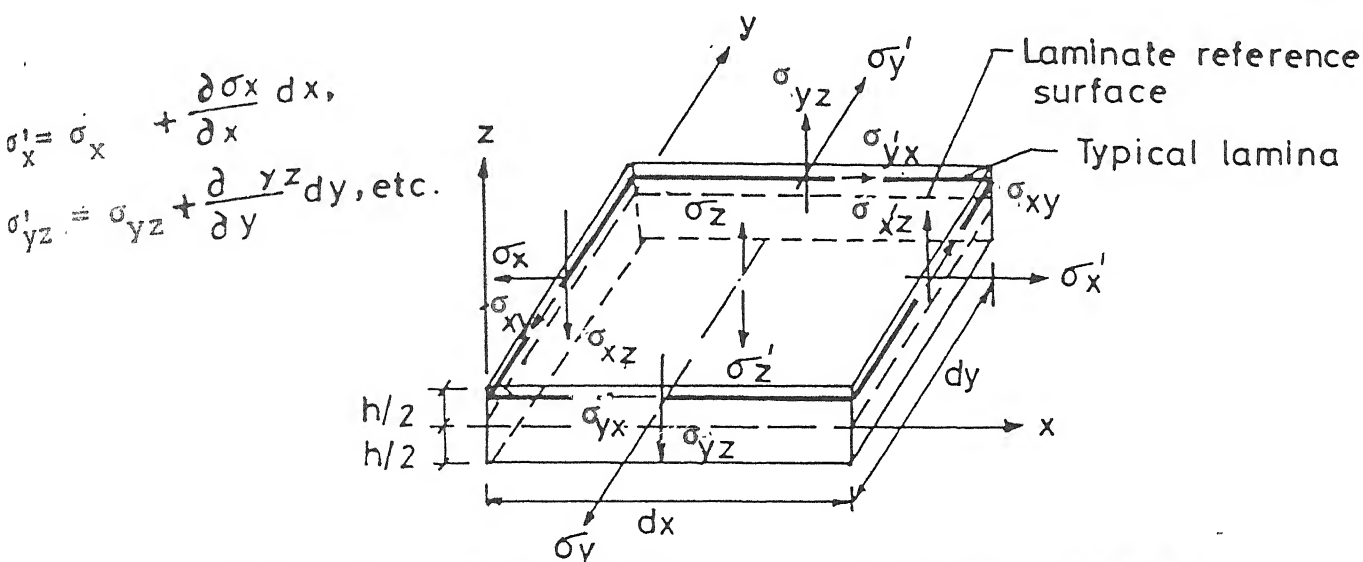
(a) STRESS COMPONENTS IN A TYPICAL LAMINA

$I'_x = N_x + \dfrac{\partial N x}{\partial x} dx,$

$I' = S_y + \dfrac{\partial Sy}{\partial y} dy, etc.$
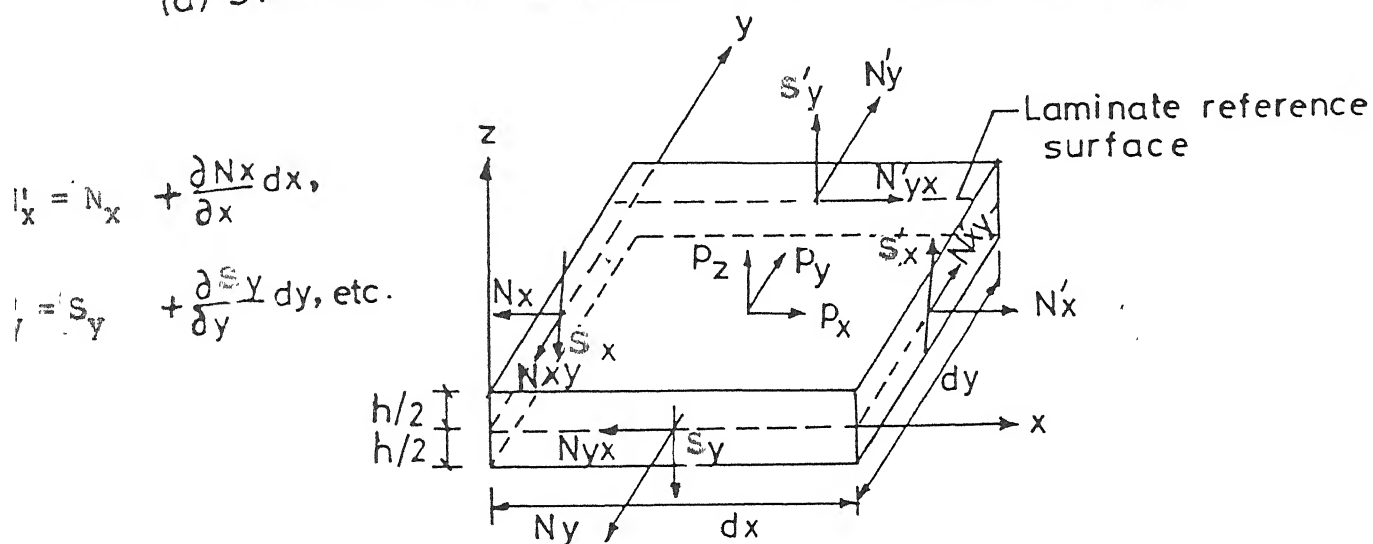
(b) STRESS-RESULTANT COMPONENTS (FORCES)

$M'_x = M_x + \dfrac{\partial M x}{\partial x} dx,$

$I'_{xy} = M_{xy} + \dfrac{\partial M xy}{\partial x} dx \; etc.$

(c) STRESS-RESULTANT COMPONENTS (COUPLES)

Fig. 4.1   POSITIVE SET OF LAMINA STRESSES AND LAMINATE
STRESS RESULTANTS (FORCES AND COUPLES)
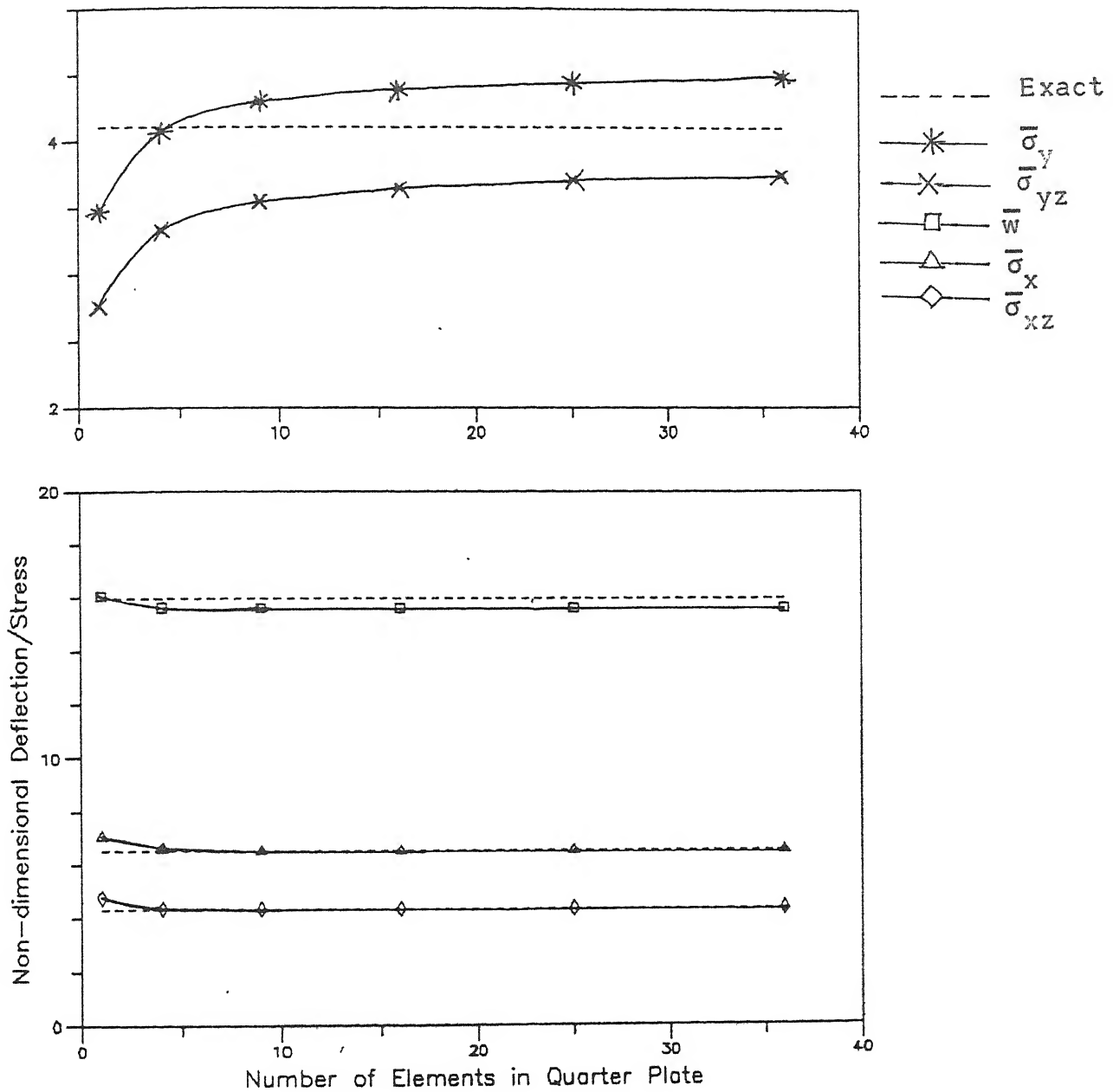
FIG. 4.2 CONVERGENCE WITH MESH REFINEMENT FOR A S.S.
3-LAYER ORTHOTROPIC LAMINATE
(UNIFORMLY DISTRIBUTED LOADING; $a/b=1$)
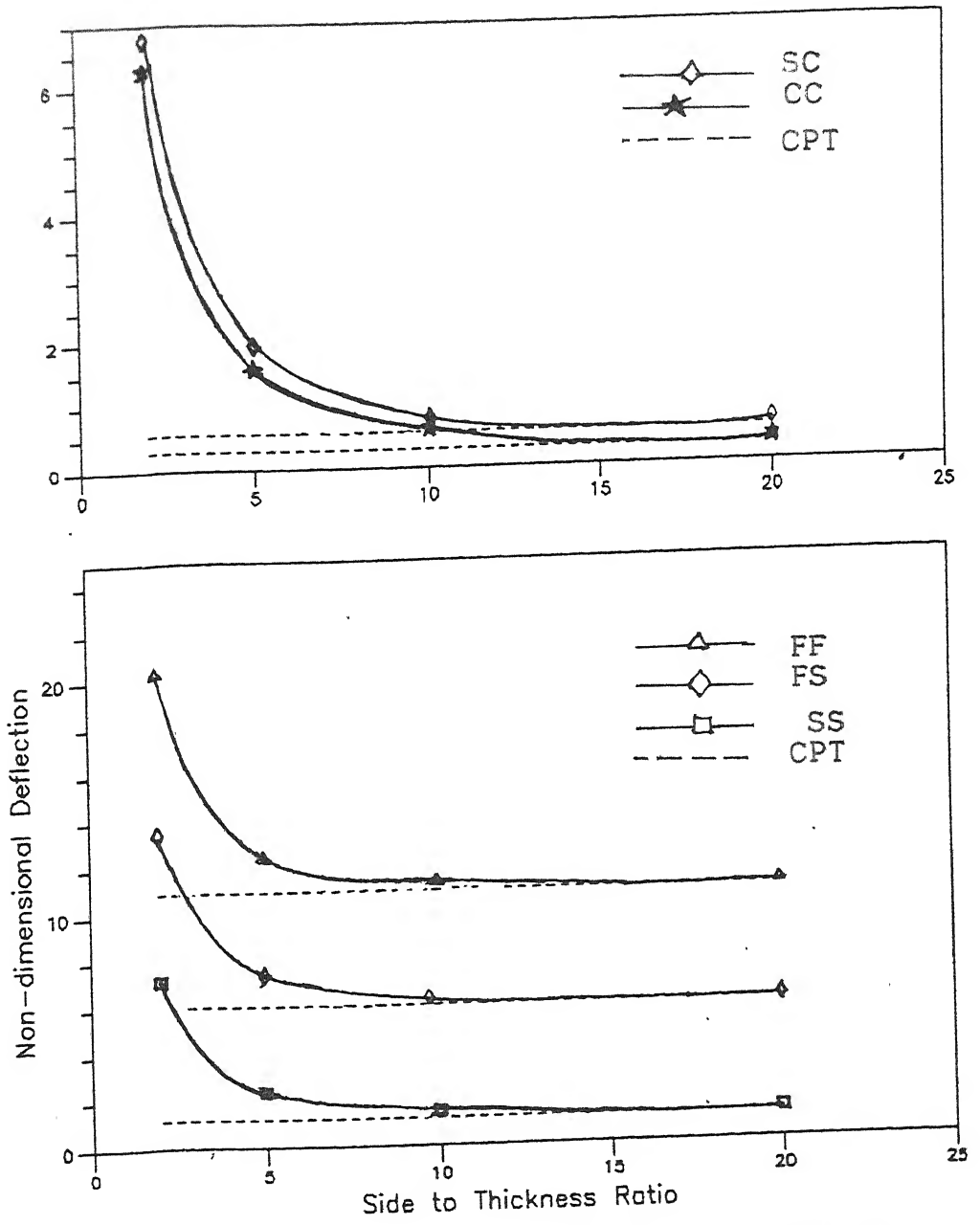
FIG. 4.3 VARIATION OF MAXIMUM CENTRAL DEFLECTION OF SYMMETRIC CROSS—PLY LAMINATE FOR VARIOUS BOUNDARY CONDITIONS (UNIFORMLY DISTRIBUTED TRANSVERSE PRESSURE; a/b=1)
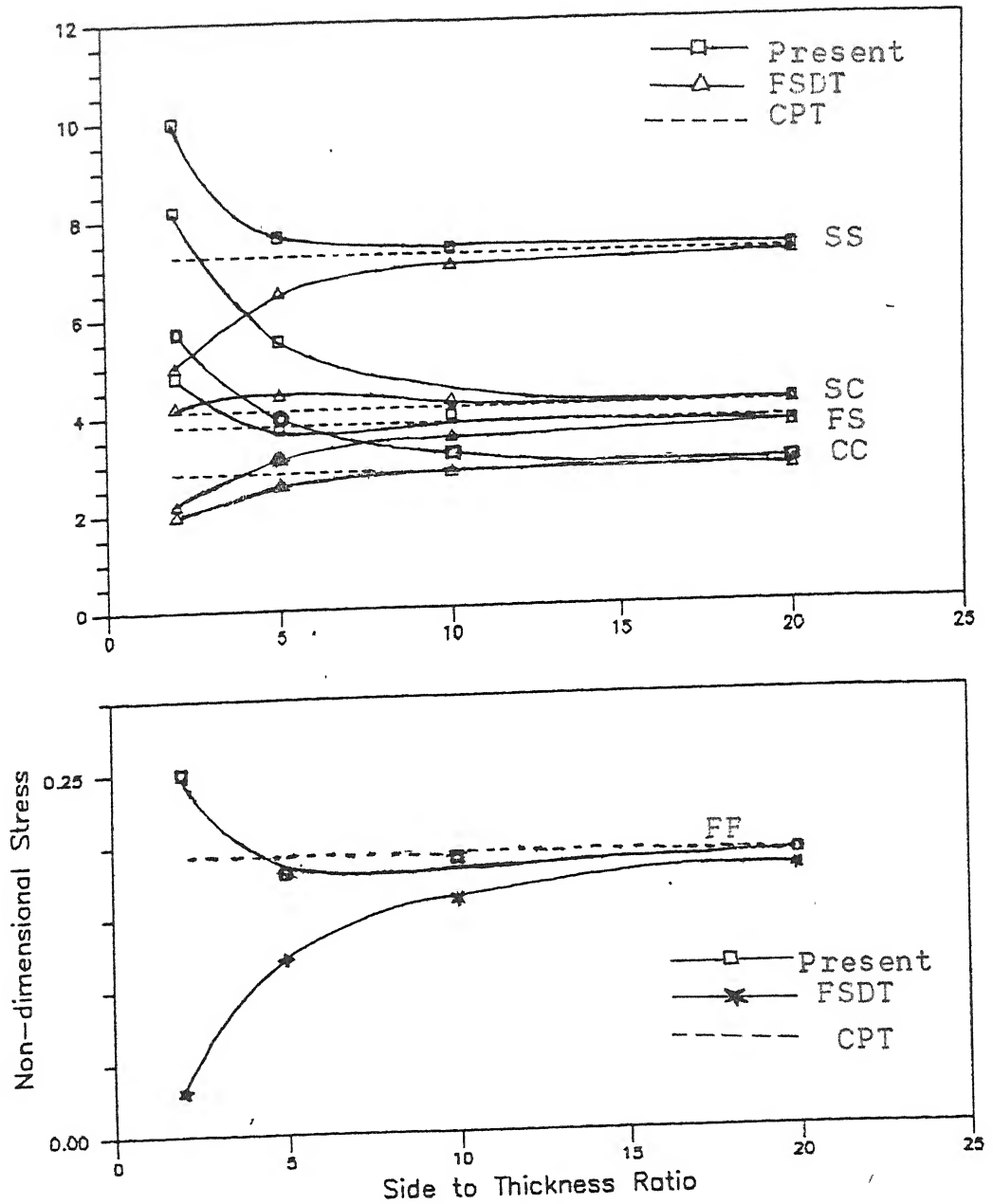
FIG. 4.4 VARIATION OF MAXIMUM INPLANE STRSS ($\overline{\sigma_x}$) OF SYMMETRIC CROSS-PLY LAMINATE FOR VARIOUS BOUNDARY CONDITIONS (SUBJECTED TO UNIFORM TRANSVERSE PRESSURE; a/b=1)
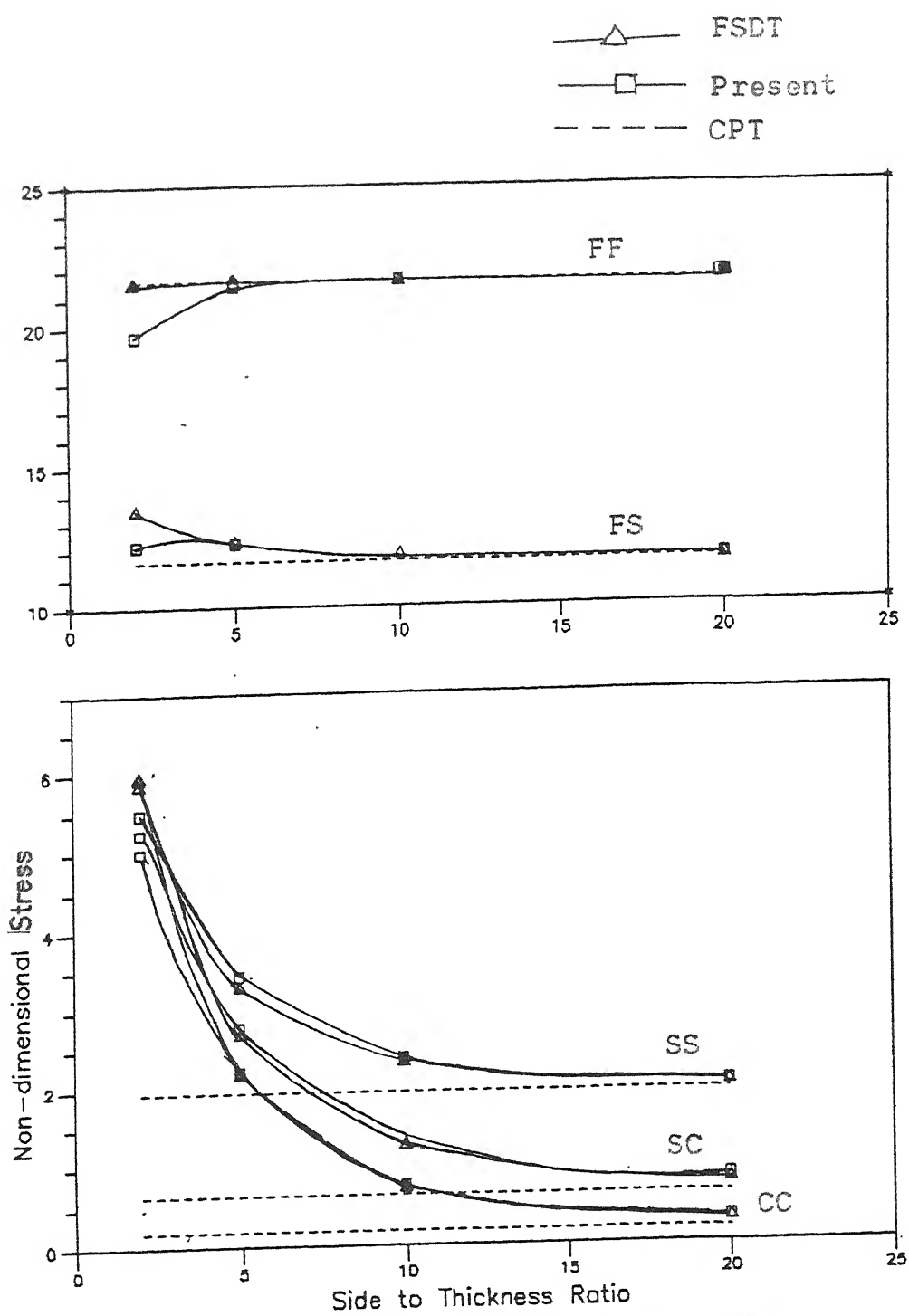
FIG. 4.5 VARIATION OF MAXIMUM INPLANE STRSS ($\overline{\sigma}_y$) OF SYMMETRIC CROSS-PLY LAMINATE FOR VARIOUS BOUNDARY CONDITIONS (UNIFORMLY DISTRIBUTED TRANSVERSE PRESSURE; a|b=1)
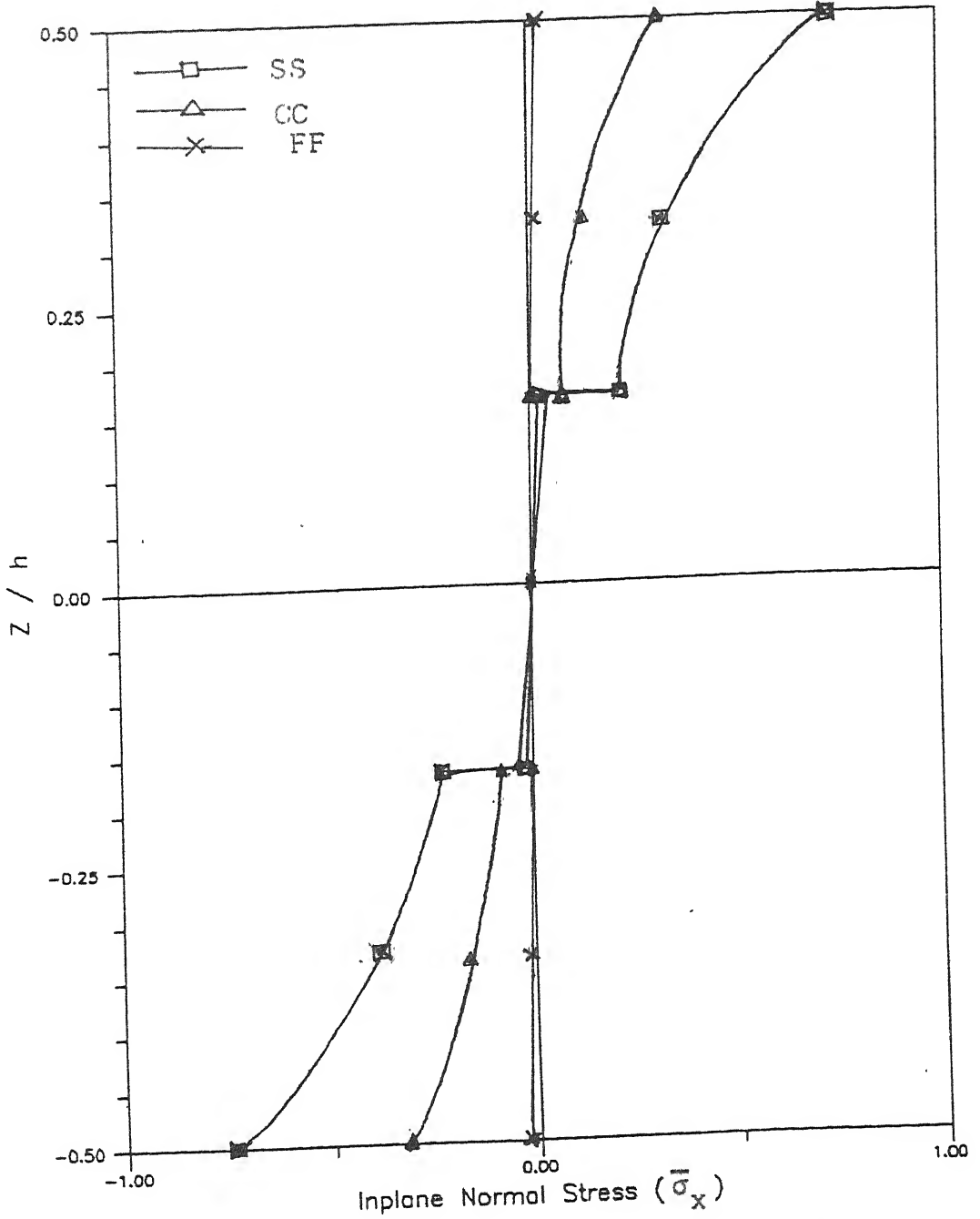
FIG. 4.6 VARIATION OF MAXIMUM INPLANE STRESS $(\overline{\sigma}_x)$ THROUGH THE LAMINATE THICKNESS OF SYMMETRIC CROSSPLY LAMINATE SUBJECTED TO UNIFORM TRANSVERSE PRESSURE (a/b=1)
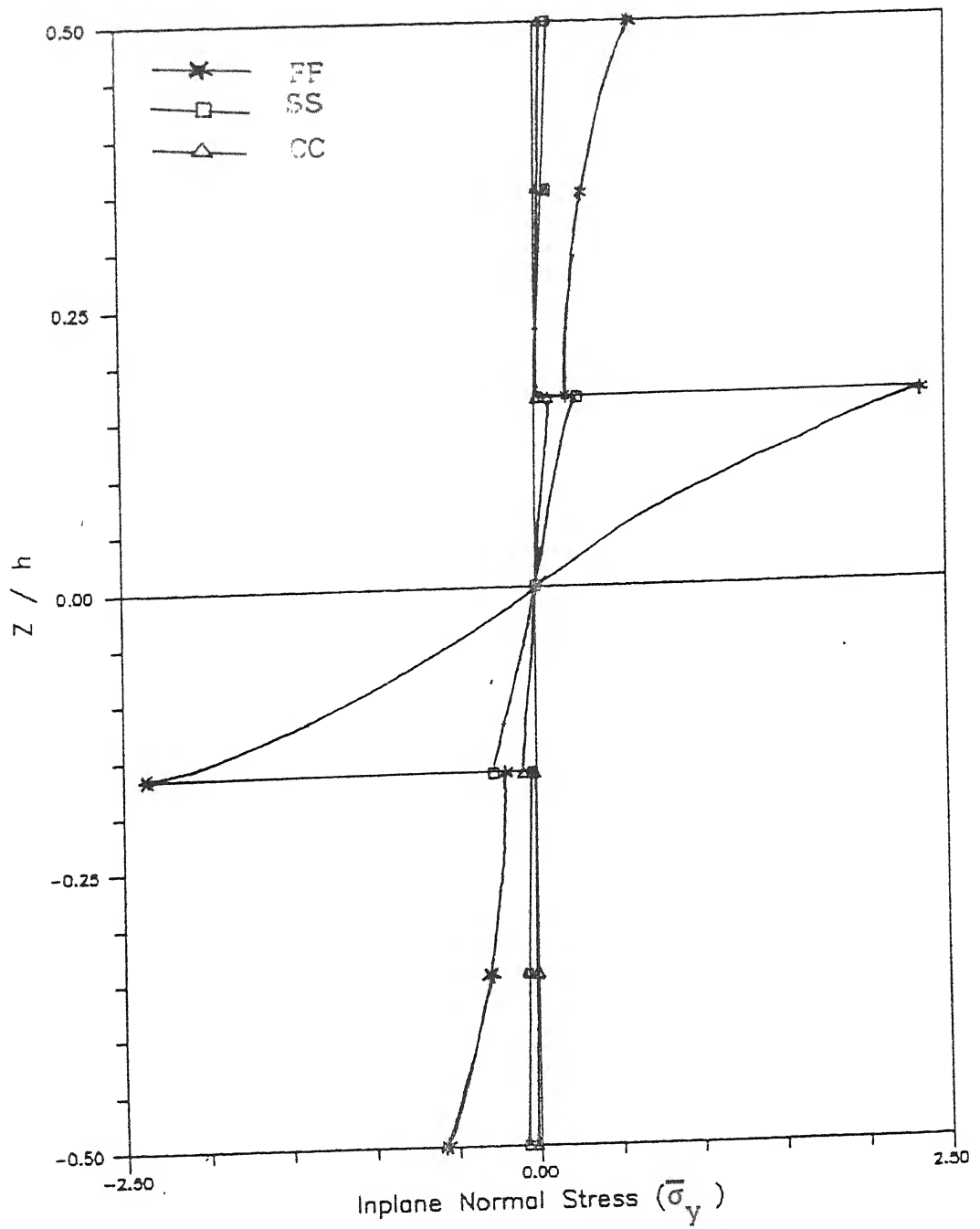
FIG. 4.7 VARIATION OF MAXIMUM INPLANE NORMAL STRESS ($\overline{\sigma}_y$)
THROUGH THE LAMINATE THICKNESS OF SQUARE
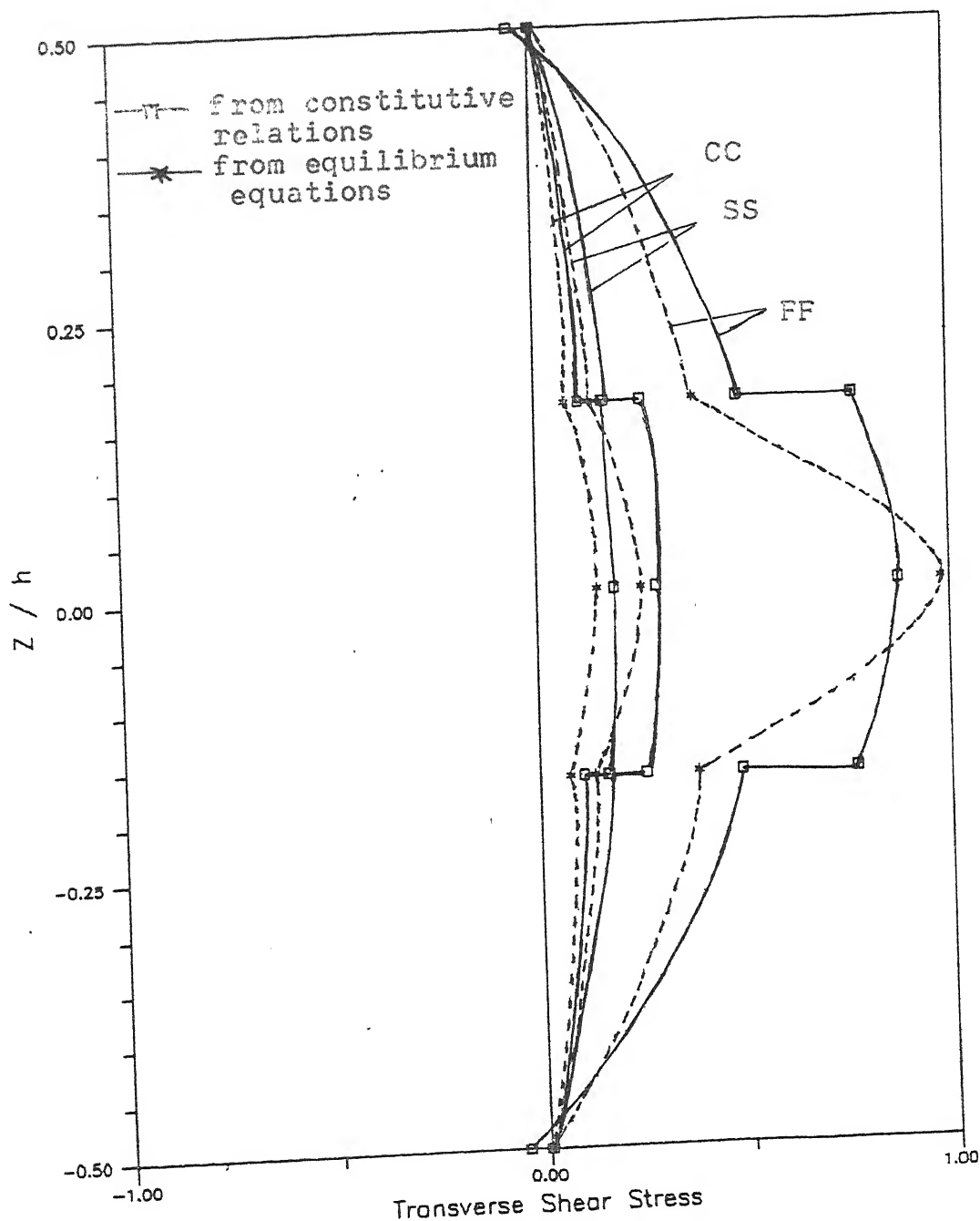SYMMETRIC CROSSPLY LAMINATE
SUBJECTED TO UNIFORM TRANSVERSE
PRESSURE.

FIG. 4.8 VARIATION OF TRANSVERSE SHEAR STRESS ($\bar{\sigma}_{yz}$) THROUGH THE LAMINATE THICKNESS OF SQUARE SYMMETRIC CROSSPLY LAMINATE SUBJECTED TO UNIFORM TRANSVERSE PRESSURE.
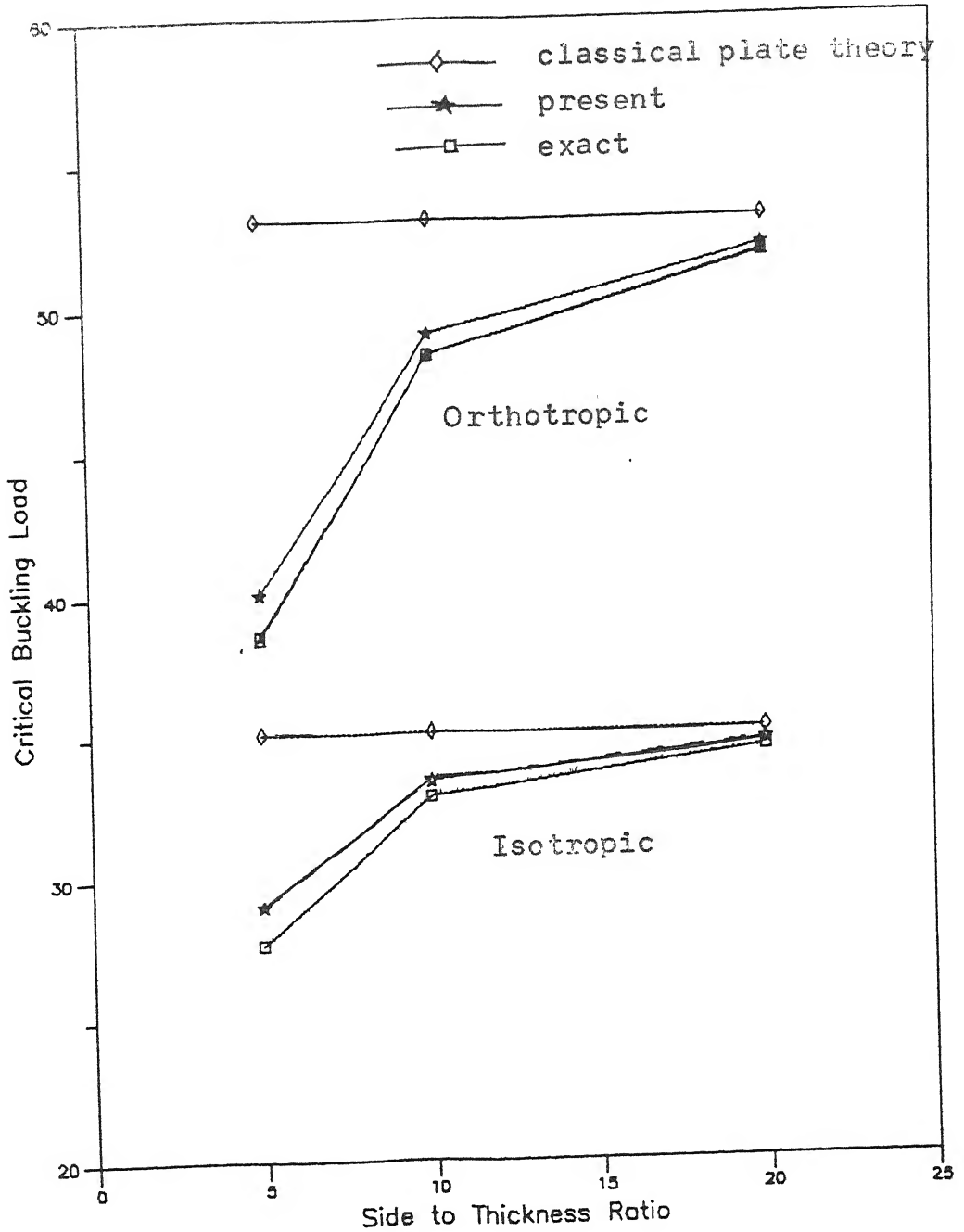
FIG. 4.9   VARIATION OF NON-DIMENSIONAL CRITICAL
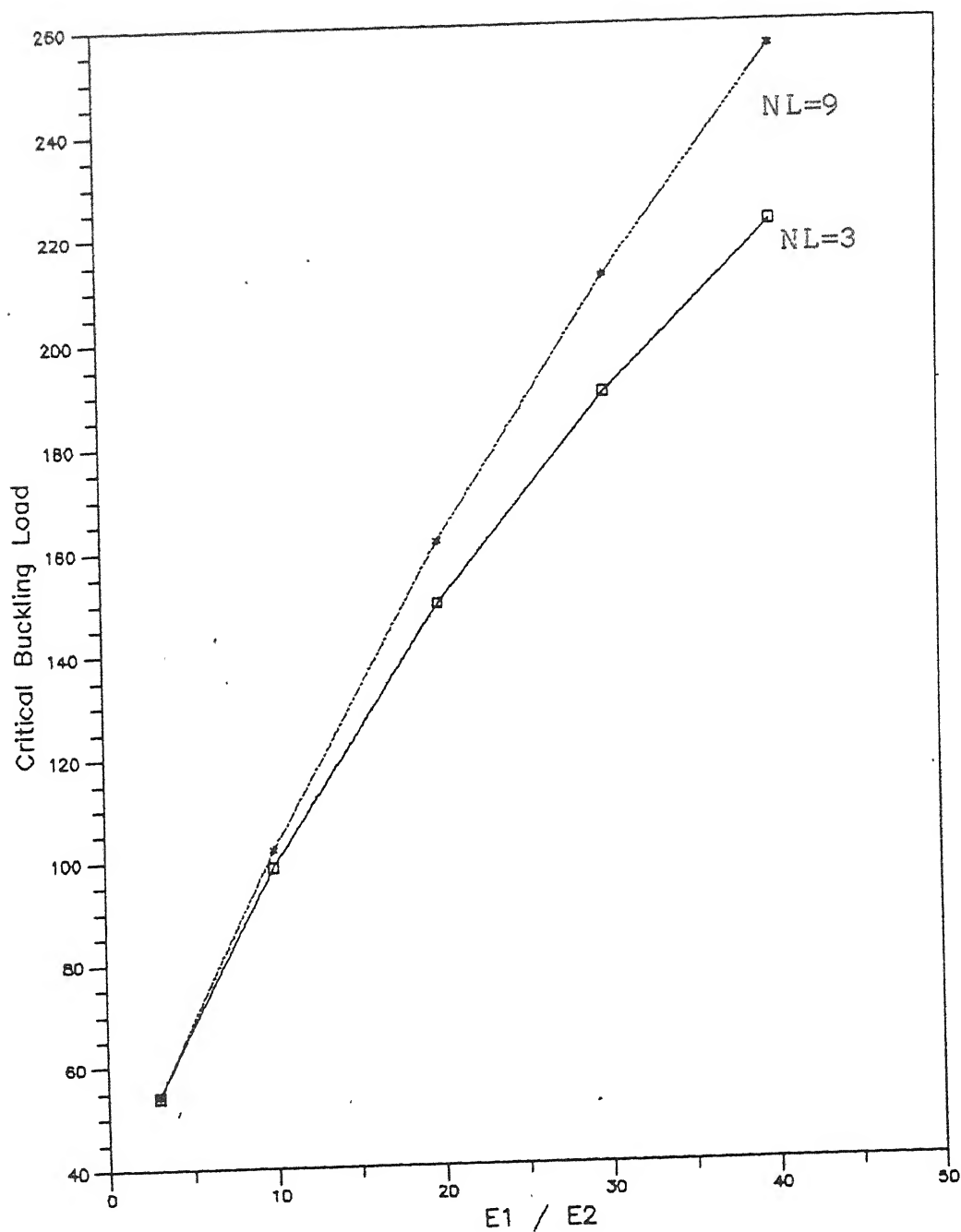BUCKLING LOAD , $\overline{N}_{cr}$ WITH SIDE TO THICKNESS RATIO
$(a/b=1)$

FIG. 4.10   VARIATION OF NON-DIMENSIONAL UNIAXIAL
BUCKLING LOAD OF SQUARE SYMMETRIC
CROSSPLY LAMINATE.

REFERENCES

1. E. Reissner and Y. Stavsk., 'Bending and stretching of
    certain types of heterogeneous aelotropic elastic plates'
    J. Appl. Mech., ASME, 28 (1961), 402-408.

2. R.D. Mindlin, 'Influence of rotatory inertia and shear on
    flexural motions of isotropic, elastic plates', J. Appl.
    Mech., ASME, 12 (1945), 1769-1777.

3. E. Reissner, 'The effect of transverse shear deformation
    on the bending of elastic plates', J. Appl. Mech., ASME,
    18 (1951), 31-38.

4. P.C. Yang, C.H. Norris and Y. Stavsky, 'Plastic wave propa
    gation in heterogeneous plates', Int. J. Solids Struct.
    2 (1966), 665-684.

5. J.M. Whitney and N.J. Pagano, 'Shear deformation in hetero
    geneous anisotropic plates', J. Appl. Mech., ASME, 37 (1970
    1031-1036.

6. J.N. Reddy, 'A penalty plate bending element for the analy
    sis of laminated anisotropic composite plates', Int. J.
    Num. Meth. Engg. 15 (1980), 1187-1206.

7. J.N. Reddy and W.C. Chao, 'A comparison of closed form and
    finite element solutions of thick anisotropic rectangular
    plates', Nucl. Engg. Des. 64 (1981), 153-167.

8. J.N. Reddy, 'A note on symmetry considerations in the
    transient response of unsymmetrically laminated anisotropic
    plates', Int. J. Num. Meth. Engg. 20 (1984), 175-194.

9.   Tagblou and Ochoa, 'Finite element formulation including interlaminar stress calculations', Computers and Structures, 23, No.2 (1986), 241-249.

10. N.G.R. Iyengar and J.R. Umaretiya, 'Deflection analysis of hybrid laminated composite plates', Composite Struct., 5 (1986), 15-32.

11. D.J. Haas and S.W. Lee, 'A nine noded assumed strain finite element for composite plates and shells', Computers and Structures, 26, No.3 (1987), 445-452.

12. D.R.J. Owen and Z.H.Li, 'A refined analysis of laminated plates by finite element displacement methods-I. Fundamentals and static analysis', Computers and Structures, 26, No.6 (1987), 907-914.

13. Lo K.H., R.M. Christensen and E.M. Wu, 'A higher order theory of plate deformation', Parts 1 and 2, J. Appl. Mech., ASME, 44 (1977), 663-676.

14. E. Reissner, 'On transverse bending of plates, including the effects of transverse shear deformation', Int. J. Solids Struct., 11 (1975), 569-573.

15. J.N. Reddy, 'A simple higher order theory for laminated composite plates', J. Appl. Mech., ASME, 51 (1984),745-752.

16. N.D. Phan and J.N. Reddy, 'Analysis of laminated composite plates using a higher order shear deformation theory', Int. J. Num. Meth. Engg., 21 (1985), 2201-2219.

17. N.S. Putcha and J.N. Reddy, 'A refined mixed shear flexible finite element for the nonlinear analysis of laminated plates', Computers and Structures, 22, No.4, (1986), 529-538.

18. J.G. Ren, 'Bending of simply supported, antisymmetrically laminated rectangular plates under transverse loading', Comp. Sci.,Tech. 28(1987), 231-243.

19. A.V. Krishnamurthy, 'Flexure of composite plates', Composite Struct. 7 (1987), 161-177.

20. A.V. Krishnamurthy and Vellia Chamy S., 'An higher order shear deformation theory of laminated composite panels', Composite Struct., 8 (1987), 247-270.

21. K. Vijayakumar and A.V. Krishnamurthy, 'Iterative modelling for stress analysis of composite laminates', Comp. Sci. Tech., 32, No.3 (1988), 165-181.

22. L. Librescu and A.A. Khdeir, 'Analysis of symmetric cross ply laminated elastic plates using a higher order theory - Part I - stress and displacement', Composite Struct. 9 (1988), 189-211.

23. Tarun Kant, 'Transient dynamics of fibre reinforced composite plates', Final Report, ARDB Research Project, Ministry of Defence, Government of India (1987).

24. O.C. Zienkiewicz, 'The finite element method', Tata McGraw-Hill, New Delhi (1987).

25. Robert D. Cook, 'Concepts and applications of finite element analysis', John Wiley and Sons, New York (1981).

26. Kapur K.K., 'Stability of plates using the finite element method', J. Engg. Mech., ASCE (1966), 177-195.

27. W.G. Carson and R.E. Newton, 'Plate buckling analysis using a fully compatible finite element', AIAA Jl. 7 (1969), 527-529.

28. Robert D. Cook, 'Finite element buckling analysis of homogeneous and sandwich plates', Int. J. Num. Meth. Engg. 9, No. 1 (1975), 30-39.

29. H.R. Lundgren and A.E. Salama, 'Buckling of multilayer plates by finite elements', J.Engg. Mech., ASCE, EM2 (1971), 477-493.

30. N.G.R. Iyengar, 'Structural stability of columns and plates', EWP, New Delhi (1986).

31. R.M. Jones, 'Buckling and vibration of unsymmetrically laminated cross-ply rectangular plates', AIAA Jl. 11, No.12 (1973), 1626-1632.

32. J.M. Whitney, 'Curvature effects in the buckling of symmetrically laminated rectangular plates with transverse shear deformation', Composite Struct. 8 (1987), 85-103.

33. D.J. Dawe and T.J. Craig, 'The vibration and stability of symmetrically laminated composite rectangular plates subjected to inplane stresses', Composite Struct. 5 (1986), 281-307.

34. D.R.J. Owen and Z.H.Li, 'A refined analysis of laminated plates by finite element displacement methods-II'. Vibration and stability', Computers and Structures, 26, No.6 (1987), 915-923.

35. Gajbir Singh and Y.V.K. Sadasiva Rao, 'Stability of thick angle ply composite plates', Computers and Structures, 29, No.2 (1988), 317-322.

36. J.N. Reddy and N.D. Phan, 'Stability and vibration of isotropic, orthotropic and laminated plates according to a higher order shear deformation theory', J. Sound. Vib. 98 (1985), 157-170.

37. N.S. Putcha and J.N. Reddy, 'Stability and natural vibration of laminated plates using a mixed element based on a refined plate theory', J. Sound. Vib. 104, No.2 (1986), 283-300.

38. Doong, 'Vibration and stability of an initially stressed laminated plate based on a higher order deformation theory', Composite Struct. 7 (1987), 285-310.

39. A.A. Khdeir, 'Free vibration and buckling of symmetric cross ply laminated plates by an exact method', J. Sound. Vib. 126, No.3 (1988), 447-461.

40. A.A. Khdeir, 'Free vibration and buckling of unsymmetric cross ply laminated plates using a refined theory', J. Sound. Vib. 128, No.3 (1988), 377-395.

41. J.G. Ren and D.R.J. Owen, 'Vibration and buckling of laminated plates', Int. J. Solids. Struct. 25, No.2 (1989), 95-106.

42. A.K. Noor and W.S. Burton, 'Assessment of shear deformation theory for multilayered composite plates', Applied Mech. Reviews, 42, No.1 (1989), 1-13.

43. K.J. Bathe and E.L. Wilson, 'Numerical methods in finite element analysis', Prentice Hall, New Delhi (1987).

44. Srinivas, S. and Rao, A.K., 'Bending, vibration and buckling of simply supported thick orthotropic plates and laminates', Int. J. Solids Struct. 6 (1970), 1463-1481.

45. Kuo Taiyen, 'Deflections of a simply supported, rectangular sandwich plate subjected to transverse loads', NACA TN 2581 (1950-1951).

46. H.G. Allen, 'Analysis and design of structural sandwich panels', Pergamon Press, London (1969).

47. Kanematsu and Hirano, 'Bending and vibration of CFRP faced rectangular sandwich plates', Composite Struct. 10, No.2 (1988).

48. Noor, A.K., 'Stability of multilayered composite plates', Fibre Sci. Tech. 8, No.2 (1975), 81-89.

APPENDIX

COMPUTER IMPLEMENTATION

A FORTRAN implementation of the present formulation is
used to solve a variety of numerical examples. Programmes have
been separately written for bending and buckling cases. Sepa-
rate routines are written to generate the stiffness matrices
for symmetric and asymmetric laminates and stored in separate
files, any of which may be run along with the main file depend-
ing on the problem. The separate formulation and program for
the symmetric laminate brings down the CPU time to a quarter of
that for an unsymmetric laminate.

In view of the large matrices that would be involved, the
global, stiffness matrices are stored in a compact form using
the profile (skyline) storage technique. In this technique,
coefficients of the global stiffness matrix within the non-
zero profile of the matrix only are stored. This always requires
less storage than a banded storage. Secondly, the storage re-
quirements are not severely affected by a few very long columns.

The procedure involves the calculation of the number of
equations to be solved after eliminating the equations with
prescribed displacements. The equation number for each degree
of freedom of each node is assigned. Then, using the elemental

connectivity and equation numbers, the column heights above the principal diagonal are calculated. Using these column heights, positions of diagonals in the single subscript array for the stiffness matrix storage are determined. This acts as a pointer array with the aid of which the actual location of any other coefficients stored in the compact array can be decided.

The Gauss elimination is used for the solution of the simultaneous equations that arise in the stress analysis. The subroutine COLSOL available in Ref. 43 which operate on the stiffness matrix stored in compact forms is used.

The solution for the eigenvalue problem that arises in the stability analysis is obtained using the subspace iteration method. The subroutine SSPACE listed in Ref. 43 is used to implement this method in conjunction with the profile storage. The routine yields the specified number of lowest eigenvalues and the corresponding eigenvectors.